SI Appendix

Simultaneous Targeting of Peripheral and Brain Tumors with a Therapeutic Nanoparticle to Disrupt Metabolic Adaptability at Both Sites

Akash Ashokan,[a,b§] Shrita Sarkar,[a,b§] Mohammad Z. Kamran,[a,b§] Bapurao Surnar,[a,b§] Akil A. Kalathil,[a] Alexis Spencer,[a] and Shanta Dhar[a,b,c]*

[a]NanoTherapeutics Research Laboratory, Department of Biochemistry and Molecular Biology, University of Miami Miller School of Medicine, Miami, FL 33136
[b]Sylvester Comprehensive Cancer Center, University of Miami Miller School of Medicine, Miami, FL 33136
[c]Department of Chemistry, University of Miami, Coral Gables, FL 33146

[§]Equally contributed authors

**To whom correspondence should be addressed.*

Email: shantadhar@med.miami.edu

Materials

Chemicals

All chemicals were used as received without further purification unless otherwise noted. Etomoxir (E1905-5MG), 2-Cyano-3-(1-phenyl-1H-indol-3-yl)-2-propenoic acid (UK-5099) (PZ0160-5MG), Bis-2-(5-phenylacetamido-1,3,4-thiadiazol-2-yl)ethyl sulfide (BPTES) (SML0601-5MG), oligomycin (O4876-25MG), carbonyl cyanide 4-(trifluoromethoxy)phenylhydrazone (FCCP) (C2920-50MG), rotenone (R8875-1G), antimycin-A (A8674-50MG), 2-deoxy-D-glucose (D8375-5G) Cisplatin (15663-27-1), 6-bromohexanoic acid (4224-70-8), polyethylene glycol (HO-PEG_{3350}-OH), sodium azide (26628-22-8), dichloroacetic acid (79-43-6), triphenylphosphine(603-35-0), hydrochloric acid (320331-500ML), and nitric acid (438073-500ML) were purchased from Sigma Aldrich. PLGA-COOH of inherent viscosity dL/g, 0.15 to 0.25 was purchased from Evonik Industries. DBCO amine (A103-1G) was purchased from Click Chemistry Tools. L-Glutamine (2530081), penicillin/streptomycin (10378016), trypsin-ethylenediaminetetraacetic acid (EDTA) solution (25200056) was purchased from ThermoFisher Scientific. (2-[4-(2-hydroxyethyl) piperazin-1-yl]ethane sulfonic acid (HEPES) buffer (1 M) (15630130) and sodium pyruvate (11360070) was purchased from ThermoFisher Scientific. Dulbecco's Modified Eagle Medium (DMEM), fetal bovine serum (FBS), phosphate buffered saline (1X PBS) was purchased from Gibco (reference number 10010-023). Regenerative cellulose membrane Amicon Ultra centrifugal 100 kDa filters were purchased from Merck Millipore Ltd. XF^e96 FluxPaks (SKU 102416-100) was purchased from Agilent Seahorse Bioscience. MDA-MB-231 was purchased from American Type Culture Collection (ATCC). Antibodies against *β*-Actin (ab8226), ERCC1 (ab129267), Cyclophilin A (ab41684), SIRT 1 (ab110304), SIRT 2 (ab211033), SIRT 4 (ab124521), SIRT 5 (ab259967), SIRT 6 (ab191385), SIRT 7 (ab259968), Phalloidin (ab176753), Integrin *b*1 (ab30394), GLUT1 (ab115730), rabbit firefly luciferase (ab185924), CD31 (ab9498), and secondary antibodies, goat anti-mouse Alexa Fluor® 488 (ab150113), goat anti-mouse HRP (ab205719), and goat anti-mouse HRP (ab205718) were purchased from Abcam. SIRT 3 (D22A3), SDHA (D6J9M), HKII (C64G5), Integrin *b*5 (D24A5), and TFAM (D5C8) were purchased from Cell Signaling Technology. Primary antibodies against ZO-1 (40-2200) and mouse firefly luciferase

(MA1-16880) were purchased from ThermoFisher Scientific. RIPA Lysis and Extraction Buffer (89900), TRIzol™ (15596026), Mitochondria isolation kit (89874) and DAPI Solution (62248) were purchased from ThermoFisher Scientific. The western blots were developed using Bio-Rad clarity western ECL substrate (1705061) was purchased from Bio-Rad. Protease Inhibitor Cocktail (200-664-3) was purchased from Sigma Aldrich. RNeasy Micro Kit (74004) was purchased from Qiagen. SYBR® Green Master Mix (15596026) and iScript™ (1708890) were purchased from Bio-Rad. Platinum standard (ICP-078) was purchased from Agilent Technologies. The Firefly Luciferase Lentifect™ purified lentiviral particles (catalog number: LPP-HLUC-LV105-025-C) were purchased from GeneCopoeia. Slide-A-LyzerTM MINI dialysis devices, 10K MWCO (69572) was purchased from ThermoFisher Scientific.

Instruments

Distilled water was purified by passage through a Millipore Milli-Q Biocel water purification system (18.2 MΩ) containing a 0.22 μm filter. Dynamic light scattering (DLS) measurements were carried out using a Malvern Zetasizer Nano ZS system. Cells were counted using Countess® Automated Cell Counter procured from Invitrogen life technology. Inductively coupled plasma mass spectrometry (ICP-MS) studies were performed on an Agilent 7900 ICP-MS instrument. High performance liquid chromatography (HPLC) studies were performed in an Agilent 1200 series HPLC instrument. Mitochondrial bioenergetics assays were performed on XF^{e}96 Extracellular Flux Analyzer purchased from Agilent. H&E images were taken using a Leica microscope. Confocal microscopy was performed under Olympus FluoView FV3000 confocal microscope. Western blot images were taken by Bio-Rad ChemiDoc MP instrument. RT-PCR experiments were performed in Bio-Rad CFX Real-Time PCR Detection Systems. TEM images were recorded using JEOL JEM-1400 instrument. Cell sorting was performed using FACSDiva 8.0.2 cell sorter.

Cell lines and culture conditions

MDA-MB-231 breast cancer cells were purchased from ATCC. MDA-MB-231-BR was obtained from Dr. Joan Massagué from Antibody and Bioresource Core Facility, Memorial Sloan Kettering Cancer Center. Both the cell lines were grown in DMEM medium supplemented with 10% FBS, 1X penicillin and streptomycin, 1X glutamine and sodium

pyruvate. Cell cultures were maintained in a humidified atmosphere of 5% CO_2 and at a temperature of 37 °C. Breast cancer cell line HCC1806 was obtained from ATCC. The cells were cultured at 37 °C in 5% CO_2 in Roswell Park Memorial Institute Medium (RPMI) 1640 supplemented with 10% fetal bovine serum (FBS), 1% penicillin/streptomycin, 1% HEPES and 1% sodium pyruvate. Cells were passaged once the flask becomes 80% confluent.

Animals

BALB/c Albino female mice (4-8 weeks old), BALB/c nude female mice (4-5 weeks old), and C57BL/6 male mice (13 weeks old) were purchased from Jackson Laboratory. All animals were handled in accordance with ‘‘The Guide for the Care and Use of Laboratory Animals’’ of American Association for Accreditation of Laboratory Animal Care (AAALAC), Animal Welfare Act (AWA), and other applicable federal and state guidelines. All animal work presented here was approved by Institutional Animal Care and Use Committee (IACUC) of University of Miami (UM) Miller School of Medicine. All housing, surgical procedures, and experimental protocols were approved by the IACUC Committee of UM. Animals had free access to chow diet and water during all experiments.

Methods

Synthesis of compounds: PLGA-*b*-PEG_{3350}-OH, PLGA-*b*-PEG_{3350}-TPP, TPP-$(CH_2)_5$-COOH, Platin-M, and Mito-DCA were synthesized by previously reported method by us.[1-6]

Synthesis of Nanoparticles: The Platin-M loaded targeted nanoparticles (T-Platin-M-NPs) and non-targeted nanoparticles (NT-Platin-M-NPs) were made using PLGA-*b*-PEG_{3350}-TPP and PLGA-*b*-PEG_{3350}-OH, respectively by nanoprecipitation method. A solution of the polymer (total concentration of polymer = 10 mg/mL) along with TPP-$(CH_2)_5$-COOH (1 mg/mL,10% feed with respect to polymer), Platin-M (2 mg/mL, 20% feed with respect to polymer), and PLGA-COOH (3 mg/mL, 30% feed) was made in 1 mL of DMF. Targeted Mito-DCA loaded nanoparticles (T-Mito-DCA-NPs) were made using PLGA-*b*-PEG_{3350}-TPP (for targeted nanoparticles 10 mg/mL); non-targeted Mito-DCA nanoparticles (NT-Mito-DCA-NPs) were constructed using PLGA-*b*-PEG_{3350}-OH with 10% TPP hexanoic acid (1 mg/mL) and 20% Mito-DCA (2 mg/mL) in 1 mL DMF following nanoprecipitation method under acidic condition. In each preparation, the DMF solution

containing the payload and polymer was added dropwise to 10 mL of deionized water with constant stirring (900 RPM) at room temperature and stirred for 2 h. The NPs were washed 3 times with nano pure water with Amicon ultracentrifugation filtration membranes with a molecular weight cutoff of 100 kDa (2800 rpm, 4 °C). The formed NPs were suspended in water and stored at 4 °C. The NP size ($Z_{average}$ diameter, nm), PDI, and surface charge (zeta potential, mV) were obtained from three independent measurements. Amounts of encapsulated Platin-M and Mito-DCA inside the polymeric nanoparticles were quantified by measuring the contents of Pt by ICP-MS and Mito-DCA by HPLC, respectively. The morphology of the NPs was evaluated using TEM. NPs at a concentration of 5 mg/mL with respect to the total polymer were diluted 100 times using nanopure water. This NP solution (1 mL) was mixed with a 4% solution of uranyl acetate solution (10 μL) and gently vortexed. This solution was filtered with a 0.45 μm filter and ~20 μL was dropped on the dark side of a copper grid and allowed to dry for 24 h in a desiccator at room temperature. TEM images were recorded using a JEOL JEM-1400 instrument.

Stability of T-Platin-M-NP and T-Mito-DCA-NP: The stability study of the nanoparticles was conducted by monitoring the size and zeta potential of the nanoparticles over a period of 10 days while storing them at 4 °C. T-Platin-M-NP and T-Mito-DCA-NP were prepared at concentration of 10 mg/mL with respect to the polymer. The size and zeta potential of the nanoparticles were measured. The nanoparticle solutions were made into 100 μL aliquots and stored at 4 °C. The size and zeta potential of the nanoparticle aliquots were measured after predetermined intervals of days using Zetasizer instrument.

Release Kinetics of Platin-M and Mito-DCA from Nanoparticles: The release of Platin-M from T-Platin-M-NPs and Mito-DCA from T-Mito-DCA-NP was studied using 1X PBS at physiological pH of 7.4 at 37 °C. Respective nanoparticle solutions were prepared at a concentration of 2 mg/mL with respect to the polymer and 200 μL of this nanoparticle solution was added into dialysis tubes with molecular Weight cut off of 10,000 Da. These tubes with nanoparticle solutions were submerged in PBS at pH 7.4 and kept under stirring in an incubator at 37 °C up to 72 h. For the first 8 h, buffer was replenished with fresh buffer every hour and later changed every 12 h. The samples were collected at

predetermined time points and samples were analyzed by ICP-MS and HPLC to determine the amount of Platin-M and Mito-DCA, respectively.

Cellular Fractionation of Cells Treated with Platin-M-NPs, Platin-M, and Cisplatin: MDA-MB-231-BR cells were plated at a concentration of 1.0 x 10^6 in 10 mL of media in a T-75 flask and allowed to grow overnight. Cisplatin (10 μM), Platin-M (10 μM), T-Platin-M-NPs, or NT-Platin-M-NPs (For NPs, concentrations used are 10 μM with respect to Platin-M) were added to cells and incubated for 12 h. After 12 h, the mitochondria and the cytosol fractions were isolated using a mitochondria isolation kit for mammalian cells. Cells were isolated by trypsinization followed by washing with 1X PBS 3 times. Reagent A (800 μL) was added followed by incubation on ice for 2 min. Reagent B (10 μL) was added and incubated on ice for 5 min with gentle vortexing every min. Following this, reagent C was added, and the cells were centrifuged (700xg at 4 °C for 10 min). The resulting pellet yielded the nuclei and cellular debris. The supernatant, containing the cytosolic and mitochondrial fractions, was removed and further centrifuged (12,000xg at 4 °C for 15 min). The resulting supernatant contained the cytosolic fraction, and the pellet contained the impure mitochondrial fraction. This was further purified by washing with reagent C and centrifuging at 12,000xg at 4 °C for 5 min. The isolated nuclei and cellular debris were further fractionated to obtain a pure nuclear fraction. The pellet was resuspended in 600 μL of a modified Tris-HCl buffer (10 mM Tris-HCl, pH 7.0, 10 mM NaCl, 3 mM $MgCl_2$, 30 mM sucrose) and incubated on ice for 10 min and then centrifuged (3000 rpm, 4 °C). The resulting pellet was resuspended in 1 mL of prechilled $CaCl_2$ buffer (10 mM Tris-HCl of pH 7.0, 10 mM NaCl, 3 mM $MgCl_2$, 30 mM sucrose, 10 mM $CaCl_2$). This was repeatedly centrifuged and washed with the $CaCl_2$ buffer, and the supernatant was discarded every time. The pellet was further purified by resuspending in a buffer of 20 mM Tris-HCl of pH 7.9, 20% glycerol, 0.1 M KCl, and 0.2 mM EDTA and centrifuging at 14,000 rpm for 30 min at 4 °C. The resulting pellet yielded the purified nuclear fraction and was resuspended in H_2O. The amount of protein in each fraction was analyzed by a BCA assay and the Pt content of each fraction was quantified by ICP-MS.

Quantification of mtDNA-Pt and nDNA-Pt Adducts: The mitochondria and nuclei were isolated according to the protocols mentioned before. For mitochondrial DNA (mtDNA) isolation, the freshly isolated mitochondria were re-suspended in 35 μL of mitochondrial

lysis buffer. To this, 5 μL of the enzyme mix was added. This was incubated at 50 °C in water bath until it became clear solution (~1 h). Absolute ethanol (100 μL) was added, and the resulting solution was incubated for 10 min at -20 °C. The solution was then centrifuged at 14000 rpm for 5 min at room temperature. The obtained pellet was further purified by washing with 70% ethanol in nanopure H_2O. The resulting purified mtDNA was resuspended in tris-EDTA (TE) buffer and quantified for the amount and purity of DNA by UV-Vis spectroscopy (260/280 nm) and the amount of Pt by ICP-MS. For nuclear DNA (nDNA), the freshly isolated nuclei were re-suspended in 40 μL of cell lysis buffer. To this, 5 μL of the enzyme mix was added. This was incubated in a 50 °C water bath until the solution turned to clear (~1 h). Absolute ethanol (100 μL) was added, and the resulting solution was incubated for 10 min at -20 °C. The solution was then centrifuged at 14000 rpm for 5 min at room temperature. The resulting pellet was then purified by washing with 70% ethanol in nanopure H_2O. Reprecipitation with 70% ethanol in nanopure H_2O was performed until the ratio of the absorbances at 260 and 280 nm was ≥1.75 and ≤2.1. The purified nDNA was resuspended in TE buffer and was quantified for the amount of DNA by UV-Vis spectroscopy (260/280 nm) and the amount of Pt by ICP-MS.

Western Blotting: Cells were grown in 25 cm^2 flask and treated with Cisplatin (10 μM), Platin-M (10 μM), T-Platin-M-NPs, or NT-Platin-M-NPs (10 μM with respect to Platin-M) for 24 h. Cells were harvested with trypsin-EDTA and lysed with RIPA buffer to yield cell lysate. Total cell lysate was collected, and protein estimation was carried out using BCA method. For animal tissue samples, they were dounce homogenized, lysed using RIPA buffer, and protein was quantified using BCA assay. For Western blotting, 50 μg of protein was resolved on 4 -20% gradient gel. Proteins were transferred to PVDF membrane and probed and blocked in respective blocking buffer. Primary antibodies, anti-SIRT1 (1:2000), anti-SIRT2(1:1000), anti-SIRT3(1:1000), anti-SIRT4 (1:1000), anti-SIRT5 (1:1000), anti-SIRT6 (1:2000), anti-SIRT7 (1:1000), anti-Cyclophilin A (1:1000), anti-TFAM (1:2000), anti-ERCC1 (1:1000), anti-β5 (1:1000), anti-β1 (1:1000), and β-actin (1:3000) were added at mentioned dilution overnight at 4 °C. After three TBST washing, membrane was probed with HRP-conjugated anti-mouse/anti-rabbit secondary antibody (1:5000) for 1 h at room temperature. The membrane was washed three time with TBST and developed using clarity western ECL substrate. The images were taken using a

BioRad ChemiDoc MP imaging system. The bands in the membrane were quantified using the ImageJ.

RNA Sequencing: MDA-MB-231-BR cells were treated with cisplatin (10 μM) and T-Platin-M-NP (10 μM with respect to Platin-M) and trypsinized and pellets were used for genome sequence analysis. The brain tissue sample from the mice treated with saline, cisplatin, and T-Platin-M-NP+T-Mito-DCA-NP were harvested and analyzed by RNA sequencing. Below are the steps which were followed for RNA sequencing and analyses:

(1) RNA extraction protocol: The total RNA was extracted from 10 mg of each tissue sample using the manufacturer's protocol provided by Qiagen. Briefly, samples are first lysed and homogenized with RLT buffer. Ethanol was added to the lysate for providing ideal binding conditions. The lysate was then placed in Rneasy silica membrane where the RNA will bind to the silica membrane. Any contaminants from the homogenate were washed with washing buffer. The residual amount of DNA from each sample was eliminated using an on-column Dnase treatment. Finally, the pure RNA is eluted in Rnase free water and further the RNA integrity was quantified prior to performing the transcriptome sequencing. To obtain high quality sequencing data, the raw data was filtered through a series of filtration methods. Base calling was utilized to transform the original data obtained from high throughput sequencing platforms into sequenced reads.[7] The records of all raw data were kept in a FASTQ file which contains sequenced reads and their corresponding sequencing quality information. The following FASTQ format was used to store every sequenced read.

(2) Assembly and mapping to a reference genome: The filtered clean sequenced reads from all samples were mapped to a reference genome by HISAT2,[8] the position and genetic characteristics were acquired following the analysis procedure of HISAT.[9-11]

(3) Statistics of mapped read to reference genome: In an experiment, ideally it is possible to align around 60-90% of the reads to the reference genome. This number majorly depends on the quality of the sample and coverage of the reference genome. The percentage of clean reads that can be mapped to the reference genome with respect to the total number of clean reads in termed as the mapping rate. This feature can be affected by multiple factors, the genetic relationship between the sequencing species and the species with the reference genome, the quality of the assembly and the quality of

sequencing, the proximity between the species. A higher mapping rate is a result of complete reference genome assembly and high-quality sequencing reads. Further, to view the alignment and annotation files mapped between the sequence reads of the sample and the reference genome, Integrated Genomics Viewer (IGV) is recommended. A qualified transcriptomic library is a prerequisite for proper transcriptome sequencing. Thus, the library quality was evaluated for quality control.

(4) Gene expression quantitative analysis*:* The genetic expression was quantified using the hits targets the genomic region or the exon region of the gene. Expression levels are initially measured as "FPKM" or Fragments Per Kilobase of transcript per Million mapped reads. FPKM[12] is a unit of measuring expression for NGS experiments. The number of reads corresponding to a particular gene is normalized to the total number of mapped reads. It is currently the most used method in expression level calculation, the calculation formula is as follow:

$$FPKM = \frac{cDNA\ Fragments}{Mapped\ Fragments\ (Millions) x\ Transcrip\ Length\ (kb)}$$

The Cuffquant and Cuffnorm components of the Cufflinks software was used to quantify the transcripts and gene expression levels using the mapped gene's positional information on the gene. Further, the normalized data was used to measure the z-score values of individual genes in each sample to investigate the genetic distribution across the different cell lines.[13-23] The use of transcriptomic analysis to detect gene expression in samples have high sensitivity. Ideally, RPKM values that reveal protein coding genes expression can be sequenced for a span of six orders of magnitude from 10^{-2} to 10^{4}.[24] Quality Control and adapter trimming was performed with FastQC[25] and fastp.[26] The filtered clean reads were mapped to reference genome by HISAT2.[27] Htseq-count[28] was used to quantify transcripts and gene expression levels using mapped reads' positional information on the reference genome and we used DESeq[29] to analyze the Differentially Expressed Genes (DEGs) for samples with biological replicates. Functional annotation for DEGs was performed with HMMER,[29] DIAMOND,[30] EggNOG-mapper,[31] clusterProfiler[32] and KofamKOALA.[33] Gene Ontology (GO) and Kyoto Encycloepedia of Genes and Genomes (KEGG) analysis was done with clusterProfiler and KofamKOALA.

Efficacy study of T-Platin-M-NP in combination with glycolysis inhibitor, 2-DG in mouse model: The efficacy of combination therapy by T-Platin-M-NP along with a glycolysis inhibitor 2-DG was studied in xenograft mice model. The tumor mouse model was established by implanting MDA-MB-231-BR cells subcutaneously in the right flank of the mice (10^6 cells per mouse). The study was performed in N = 25 female BALB/c nude mice (4-5 weeks, Jackson laboratory). The tumor progression and body weight were monitored twice a week. Once the tumor reached 100 mm^3, the mice were randomly divided into five groups to study the efficacy of combination therapy over monotherapy. The treatment groups were saline (n = 5), cisplatin (n = 5) at a dosage of 5 mg/kg, 2-DG (n = 5) at dosage of 5 mg/kg, T-Platin-M-NP (n = 5), at a dosage of 5 mg/kg with respect to Platin-M, and a combination of T-Platin-M-NPs + 2-DG (n = 5) at a dosage of 5 mg/kg with respect to Platin-M and 5 mg/kg of 2-DG, respectively. Treatment was carried out biweekly *via* tail i. v. route for 4 weeks and tumor volume and body weight were constantly monitored. Animals were euthanized, organs were harvested at the end of the study, and %Pt in the brain and tumor were measured using ICP-MS in cisplatin, T-Platin-M-NP, and T-Platin-M + 2-DG treated groups. RNA sequencing of genes related OXPHOS, Glycolysis, NER, and BER pathways in the tumor samples was also performed.

Toxicity study in normal mice: The toxicity study of test articles was performed in female C57BL/6 (N = 15) mice which were purchased from Jackson laboratory (age ~6 weeks). Animals were randomized into 5 treatment groups according to their body weight which are saline (n = 3), cisplatin (n = 3) at a dosage of 3 mg/kg, 2-DG (n = 3) at dosage of 5 mg/kg, T-Platin-M-NP (n = 3), at a dosage of 5 mg/kg with respect to Platin-M, and a combination of T-Platin-M-NPs + 2-DG (n = 3) at a dosage of 5 mg/kg with respect to Platin-M and 5 mg/kg of 2-DG respectively. The treatment was carried out biweekly *via* tail i. v. route for 4-weeks period and body weight was monitored once a week. Blood from each animal were collected at the end of the study, animals were euthanized, and organs were harvested. Clinical chemistry analysis of the blood samples was carried out at cancer shared modelling resource core facility to understand the toxicity of the test articles. H&E slides were prepared by cancer shared modelling resource core facility. Brain samples from the mice were also used for western blotting to understand the levels for different sirtuins.

Migration assay: Migration assay was carried out as described previously with minor modification. MDA-MB-231 and MDA-MB-231-BR cells ($0.3x10^6$) were seeded in 6 well plate and treated with Cisplatin (10 μM), Platin-M (10 μM), T-Platin-M-NPs and NT-Platin-M-NPs (10 μM with respect to Platin-M) for 24 h. Cells were scratched with 200 μL pipette tip and washed with PBS to remove peeled off cells. At 0 h, control cells were fixed immediately with chilled methanol after scratching. Rest of the cells were incubated in 5% serum containing media for wound coverage. After 36 h, cells were washed with PBS, fixed with chilled methanol and stained with 1% crystal violet solution. Images were taken using microscope. The migration observed was represented as percentage migration.

Adhesion assay: For adhesion assay, 96-well plates were coated with Matrigel or Collagen II for 24 h at 4 °C. Plates were washed with PBS to remove unpolymerized substrates and blocked with 1% BSA for 2 h at 37 °C. Cells were treated with Cisplatin (10 μM), Platin-M (10 μM), T-Platin-M-NPs, or NT-Platin-M-NPs (10 μM with respect to Platin-M) for 24 h. Cells were harvested in media containing 1% BSA and inoculated at a density of 5×10^3 cells/well. After 1 h, cells were washed with PBS to remove non-adherent cells. The adherent cells were then determined using MTT assay.

Actin staining: MDA-MB-231 and MDA-MB-231-BR cells were seeded on coverslips and treated with Cisplatin (10 μM), Platin-M (10 μM), T-Platin-M-NPs and NT-Platin-M-NPs (10 μM with respect to Platin-M) for 24 h. Cells were washed with PBS and fixed with 4% paraformaldehyde for 10 minutes. Cells were washed twice with PBS and permeabilized with 0.1% triton X 100 for 15 minutes. After washing with PBS, cells were stained with phalloidin-fluorescein isothiocyanate mixture (50 μg/ml) for 1 h at room temperature. Cells were washed with PBS and nucleus was stained with NucBlue® (1 drop/ml) for 5 minutes. After five PBS washes, coverslips were mounted on glass slide using mounting media and edges were sealed with clear nail paint. Images were taken using confocal microscope.

Mitostress assay: MDA-MB-231 and MDA-MB-231-BR cells were seeded in XF^e96 well plate at a density of 20,000 cells per well in 50 μL DMEM media. After 6h, additional 150 μL of media was added to the cells. Cells were treated with cisplatin (10 μM), Platin-M (10 μM), T-Platin-M-NPs and NT-Platin-M-NPs (10 μM with respect to Platin-M) for 24 h. Cells were washed thrice with Seahorse basal medium and incubated at 37 °C in non-

CO_2 incubator for 45 minutes. XF sensor cartridges were hydrated using Seahorse Bioscience calibrant and kept at 37 °C in non-CO_2 incubator for a minimum of 4 h. Oxygen consumption rate (OCR) of cells were measured after addition of various inhibitors such as oligomycin (1 μM)- ATP synthase inhibitor, FCCP (1 μM)- mitochondrial membrane uncoupler, and combination of antimycin-A and rotenone (1 μM each)- complex III and I inhibitors, respectively. Oligomycin, FCCP, and the mixture of antimycin-A and rotenone were injected at 30, 60, and 90 minutes, respectively.

Glycostress assay: Glycostress assay was carried out as described in mitostress assay with minor modification. MDA-MB-231-BR cells were seeded in XF^{e}96 well plate at a density of 15,000 cells per well in 50 μL DMEM media. After 6 h, additional 150 μL of media was added to the cells. Cells were treated with cisplatin (10 μM), Platin-M (10 μM), T-Platin-M-NPs and NT-Platin-M-NPs (10 μM with respect to Platin-M) for 16 h followed by 25 μM 2-deoxy-D-Glucose (2-DG) treatment for 6 h. Cells were washed thrice with Seahorse basal medium without glucose and incubated at 37 °C in non-CO_2 incubator for 45 minutes. OCR of cells were measured after addition of various additives such as glucose (10 mM), oligomycin (1 μM), and 2-DG (50 mM) using XF^{e}96 Extracellular Flux Analyzer.

Mitostress Assay in HCC-1806 Cells: The real time OCR values through mitochondrial OXPHOS in HCC1806 cells upon treatment with NT-Platin-M-NPs and T-Platin-M-NP were determined by using Seahorse Analyzer. Different parameters of mitochondrial respiration such as basal respiration, maximal respiration, and ATP production were investigated using Seahorse XF^{e}96 Analyzer. One day prior to the assay, XF sensor cartridges were hydrated using 200 μL of XF calibrant buffer and kept at 37 °C incubator without CO_2 overnight. Cells were plated at a density of 20,000 cells per well in 80 μL RPMI media (with 10% FBS) and the plate was incubated at 37 °C with 5% CO_2 for 4 h. Finally, 100 μL of fresh media was added to have total 180 μL per well and incubated for 16 h. Cells were treated with Cisplatin (10 μM for 24 h), Platin-M (10 μM for 24 h), NT-Platin-M-NP or T-Platin-M-NP (both nanoparticles are with respect to 10 μM Platin-*C* concentration) for 4 h. After treatment, the media for nanoparticle groups were replaced with fresh media and incubated for 20 h. Before conducting the Mitostress assay, Seahorse media (XF Assay Medium Modified DMEM) was reconstituted with glucose (1.8

mg/mL), sodium pyruvate (1%) and L- glutamine (1%) and adjusted for to pH 7.4 by using 0.1 N NaOH. The cells were washed thrice with freshly prepared seahorse medium and incubated at 37 °C in non-CO_2 incubator for 1 h. Meanwhile, various reagents were added to the ports of the sensor cartridge. The port A was filled with 20 μL of oligomycin (10 μM) port B with 22 μL of FCCP (10 μM) and port C with 25 μL of antimycin A/rotenone (10 μM) to have a final concentration of 1 μM in each well. The cartridge was calibrated for pH and O_2. After calibration, the experiment plate was run where 5 measurements were recorded for basal OCR and after addition of each reagent. After the assay, the media was aspirated and 20 μL of RIPA buffer was added to each well and incubated for 20 mins at 37 °C. Further BCA assay was performed to obtain protein values and OCR values were normalized with protein concentration. The statistical analysis was obtained one-way ANOVA test.

Glycostress Assay in HCC-1806 Cells: HCC1806 cells were plated at the density of 20,000 cells/well in a 96 well plate in RPMI 1640 medium and incubated overnight in a CO_2 incubator at 37 °C. On the same day, the Seahorse XF^e96sensor cartridge in the extracellular Fuel Flex assay kit was calibrated with 200 μL of XF calibrant buffer and incubated in a non-CO_2 incubator. On the next day, the HCC1806 cells were treated with Cisplatin (10 μM for 24 h), Platin-M (10 μM for 24 h), NT-Platin-M-NP (10 μM with respect to Platin-M), or T-Platin-M-NP (10 μM with respect to Platin-M). After 4h of treatment, media was changed with fresh media for nanoparticles treated groups and incubated for 20 h. To run the pre-treated glycostress assay, the HCC1806 cells were washed three times with glucose free Seahorse medium (XF Assay Medium Modified DMEM) which contains 1% of sodium pyruvate and L- glutamine and adjusted pH value to 7.4. Then the cells were incubated in the glucose free Seahorse medium at 37 °C in a non-CO_2 incubator. For the injection, glucose (100 mM), oligomycin A (10 μM), and 2-DG (500 mM) stocks were prepared and added to port A (20 μL), port B (22 μL), and port C (25 μL), respectively. The working concentrations of glucose, oligomycin, and 2-DG were 10 mM, 1 μM, and 50 mM, respectively. After calibrating the cartridge for pH and O_2 levels, the cell plate was run in the Seahorse instrument. Four measurements of extracellular acidification rate (ECAR) were recorded before and after addition of each reagent. After completing the measurement, the medium was aspirated, and RIPA buffer (20 μL) was

added to each well and incubated for 20 min at 37 °C. The protein quantification of the cells used in glycostress assay was conducted by bicinchoninic acid (BCA) assay to normalize the ECAR values with respect to protein concentration to account for the live cells. The statistical analysis was obtained one-way ANOVA test.

Fuel Flex Assay in HCC-1806 Cells: HCC1806 cells were seeded in 96-well XF^{e}96 Seahorse microplates at a density of 20,000 cells/ well in 100 μL RPMI-1640 supplemented with 10% FBS, 1% penstrep, 1% sodium pyruvate, 1% HEPES buffer and grown for 12 h. Subsequently the media was removed again, and the cells were washed with Seahorse basal media three times and incubated at 37 °C in a non-CO_2 incubator. Fuel flex assay for the different fuel pathways viz. glucose, glutamine and fatty acid was studied by measuring the basal oxygen consumption rates and that after addition of the inhibitor of the target pathway in port A and a mixture of the inhibitors of the other two pathways in port B. This gave a measure of the dependency of the cells on a particular fuel pathway. To study the capacity of a certain fuel pathway, the sequence of addition of the inhibitors was reversed. In port A was added the mixture of inhibitors for the other pathways and in port B was added the inhibitor for the target pathway. UK-5099 (pyruvate dehydrogenase inhibitor, 2 μM) was used as an inhibitor for the glucose pathway. BPTES (selective inhibitor of Glutaminase GLS1, 3 μM) was used as an inhibitor for the glutamine pathway. Etomoxir (O-carnitine palmitoyltransferase-1 (CPT1A) inhibitor, 4 μM) was used as an inhibitor for the fatty acid pathway.

$$\% \text{ Dependency} = \left[\frac{\text{Baseline OCR -Target inhibitor OCR}}{\text{Baseline OCR- All inhibitor OCR}} \right] * 100$$

$$\% \text{ Capacity} = \left[1- \left[\frac{\text{Baseline OCR -Other 2 inhibitor OCR}}{\text{Baseline OCR- All inhibitor OCR}} \right] \right] * 100$$

$$\% \text{ Flexibilty} = \% \text{ capacity} - \% \text{ dependency}$$

Generation of Luciferase tagged MDA-MD-231BR^{Luc}cells: Two wells of a 24-well plate MDA-MD-231BR^{WT} cells were seeded at a density of 2.5 x 10^5 cells/well. The cell plate was incubated overnight at 37 °C, 5% CO_2. A solution with the luciferase lentiviral particles (GeneCopoeia, Inc.) was prepared at a ratio of 1:5 of cells to viral particles with 1 μL of polybrene. This solution of the lentiviral particles was prepared in 500 μL of DMEM growth media which was then added to the cells. This was followed by an incubation for 24 h at 37 °C, 5% CO_2. Post-transfection, the media was replenished with fresh growth media and the cells were allowed to become confluent. Once the cells reached 90% confluency, they were split into three T25 culture flasks and were allowed to grow until they became 80% confluent. Finally, the cells were exposed to the puromycin selection media (3 μg/mL) and allowed to grow for few passages until no cell death was observed. After 3 weeks of keeping the cells under puromycin selection, there was no cell death observed and the luciferase expression in the cells was confirmed by IVIS imaging.

Dual Tumor Mouse Model and T-Platin-M-NP Biodistribution: The dual tumor mouse model was established using MDA-MB-231BR^{Luc} cells where the primary tumor was implanted subcutaneously in the right flank of the mice. The secondary tumor was implanted in the brain orthotopically *via* stereotactic intracranial injection after the formation of primary tumor. The study was performed in N=14 female BALB/c nude mice (4-5 weeks, Jackson laboratory). The tumor progression was monitored by imaging the mice under IVIS once a week. Once both the primary and the secondary tumor was observed, the mice were randomly divided into three groups to further study the biodistribution of Platin-M across all the organs and tumor tissues which would be eventually harvested from these mice. The treatment groups were saline (n=5), cisplatin (n=5) at a dosage of 5 mg/kg, and a combination of T-Platin-M-NPs + T-Mito-DCA-NPs (n=4) at a dosage of 10 mg/kg with respect to Platin-M and 30 mg/kg with respect to Mito-DCA, respectively. T-Mito-DCA-NPs were injected 24 h post T-Platin-M-NP injection. All the test articles were injected twice weekly for 3 weeks *via* tail i.v. route. Since the secondary tumor was implanted in the brain, we first performed flow cytometric cell sorting of the luciferase expressing tumor cells from the brain followed by ICP-MS studies to quantify the percentage injected dose present in the respective organs, primary tumor tissue, and in the sorted tumor cells. Briefly, the whole brain was harvested post

euthanasia, collected in 5 mL of DMEM media supplemented with 10% FBS and kept on ice. Dissociation of the whole brain tissue was carried out in the biosafety cabinet. The tissue was gently minced into small pieces using a dounce homogenizer. The suspension was collected in a 15 mL centrifuge tube and centrifuged at 1500 RPM for 5 mins. To isolate the maximum number of cells from the tissue, the pellet was again dissociated with 1 mL of pre-warmed trypsin at 37 °C for 20 mins. To keep the suspension homogenous, it was agitated at a regular interval of 5 mins. Further, the trypsin was quenched by using 0.5 mL of FBS. The cell suspension was then filtered through a 100-micron cell strainer and collected in a 50 mL centrifuge tube. Additionally, 5 mL of DMEM was added dropwise on the strainer to collect maximum cells from the suspension. The filtrate was centrifuged at 1500 RPM for 5 mins and the pellet was resuspended in 1 mL of FACS buffer (2% FBS in 1X PBS). This resultant suspension was kept at room temperature for 10 mins. To ensure that we collect only the tumor cells from the whole brain cell suspension, anti-firefly luciferase antibody was used to tag the luciferase expressing tumor cells i.e., MDA-MB-231BR^{Luc} cells. After 10 mins, 5 μg of the luciferase tagged antibody was added to the whole brain cell suspension and incubated for 20 mins at 4 °C. This step was followed by incubation of the cell suspension with Alexa Fluor® 488 secondary antibody to tag the primary antibody. The suspension was then centrifuged at 1500 RPM for 5 mins and the pellet was resuspended in 0.5 mL of FACS buffer. Finally, the luciferase tagged MDA-MB-231-BR cells were sorted from the whole brain cell suspension using the FACSDiva 8.0.2 cell sorter. Prior to sorting the tumor cells from the treatment groups, we performed cell sorting on MDA-MB-231-BR^{Luc} cells with/without anti-firefly luciferase antibody incubation. MDA-MB-231-BR^{Luc} cells without antibody served as the negative control and MDA-MB-231-BR^{Luc} cells with antibody incubation served as the positive control. Further, the cells from the respective treatment groups were sorted using the positive control pattern. Cells from the similar region as the positive control were collected as the tumor cells and the remaining were collected as cells from the rest of the brain. The Pt content was further determined using ICP-MS followed by calculating the amount of NP accumulated in the brain and tumor cells. The biodistribution of Platin-M was expressed as %injected dose. The remaining organs and the tumor mass was dissolved in freshly prepared aqua regia. The organs were allowed to dissolve before

the samples were used for ICP-MS. H&E slides were prepared by cancer shared modelling resource core facility.

Efficacy study of combinatorial nanotherapy in dual tumor model: To investigate the efficacy of the combinatorial therapeutic strategy by using T-Platin-M-NP and T-Mito-DCA-NPs against breast cancer brain metastasis, we developed the dual tumor mouse model with primary tumor implanted at the right flank and secondary tumor implanted in the brain. Here, we use female BALB/c nude mice (4-5 weeks old, Jackson Laboratory) to develop the dual tumor model where we implant MDA-MB-231BR luciferase tagged cells. The MDA-MB-231BR^{Luc} cells were established from the parental triple negative MDA-MB-231BR breast cancer cells which have specific metastatic potential towards brain. We initiate the study by implanting the primary tumor (2.0×10^6 cells/mouse, 100 μL cell suspension in 1X PBS) with equal volume of Matrigel in the right flank of the mice *via* subcutaneous injection. We observed primary tumor growth in ~20 days post cell implantation. The secondary tumor was implanted in the brain after observing the primary tumor formation. Based on randomization of the animals with primary tumor, we perform orthotopic stereotactic intracranial injection and inoculated MDA-MB-231BR^{Luc} cells (1.0×10^6 cells/mouse, 2 μL cell suspension in 1X PBS) in the brain of the mice. The primary and secondary tumor progression were observed using IVIS imaging at regular time intervals. Post the secondary tumor implantation, both the primary and secondary tumors were allowed to proliferate for about 20 days before we started administering the animals with our combinatorial nanoparticles. Prior to initiating the 4-week treatment regimen, the mice were randomly divided into 3 groups. The groups were saline (n=3); cisplatin (n=4) at a dosage of 5 mg/kg; a combination of T-Platin-M-NP and T-Mito-DCA-NP (n=7) at a dosage of 10 mg/kg with respect to Platin-M and 30 mg/kg with respect to Mito-DCA, respectively. All the test articles were injected biweekly *via* intravenous route. The T-Mito-DCA-NPs was injected 24 h post T-Platin-M-NP injection. The tumor proliferation across the different groups was monitored using IVIS imaging over 4 weeks of treatment regimen. All organs and tumor tissues were harvested from the animals when either the animal did not survive or at the completion of the treatment regimen. The tumor implanted brain sections that were harvested from the mice were further used for RNA sequencing analyses and *ex-vivo* histological analyses.

Immunofluorescence analyses in tissue sections. We perform immunofluorescence in brain sections from normal BALB/c nude mice and orthotopically implanted BALB/c nude mice to observe whether the orthotopic implantation led to a disruption in blood brain barrier (BBB) integrity, where we stain the tissue for CD31 and ZO-1. In addition, we also

perform immunofluorescence analyses on primary tumor and secondary brain tissue sections of mice that were harvested post completion of the therapeutic efficacy study. The tissues were sectioned, and paraffin embedded on glass slides for further histological analyses. These primary tumor tissues were stained for sirtuins 1-7, oxidative phosphorylation (OXPHOS) related protein succinate dehydrogenase (SDHA), and glycolytic proteins hexokinase 2 (HKII) and glucose transporter 1 (GLUT1). The secondary brain tumor tissue sections were stained for sirtuin 3 (SIRT3), SDHA, HKII, and GLUT1. To closely investigate the relative change in protein expression of the above-mentioned markers, we specifically focused on the cancer cells in the brain which were stained with luciferase antibody. We use luciferase antibody to mark the MDA-MB-231-BR^{Luc} cells in the brain. Thus, we measure the effect of the test articles in the cancer cells. Briefly, the slides with the paraffin embedded tissue sections were heated at 55-60 °C for 30 mins followed by rehydration in a gradually decreasing ethanol gradient. At each step the slides were kept in the solution for 10 mins. The sequence was as follows: xylene, 100% ethanol, 95% ethanol, 80% ethanol, 70% ethanol, 60% ethanol, 50% ethanol, 40% ethanol, 30% ethanol, 20% ethanol, 10% ethanol, and finally water. The tissues were then incubated in an antigen retrieval buffer (2.94 g trisodium citrate in 1 L de-ionized water, pH adjusted to 6.0, and 500 μL of Tween-20) for 20 mins in a decloaking chamber at 95 ºC, 20 psi. The tissues were washed thrice with 1X PBS and were then subjected to permeabilization for 10 mins at room temperature. The permeabilization solution was prepared using 0.1% Triton-X-100 in 1X PBS. The tissues were again washed three times with 1X PBS and blocked with blocking buffer overnight at 4 °C. The blocking buffer was prepared using 5% goat serum in PBST for all the antibodies. All the primary antibodies were diluted in 1% BSA containing PBST. The tissues were further incubated with the primary antibody solution in a humidifying chamber overnight at 4 °C. The concentrations for each antibody were as follows; ZO-1 at 5 μg/mL, CD31 at 1:100, SIRT1 at 1:1000, SIRT2 at 1:100, SIRT3 at 1:100, SIRT4 at 1:100, SIRT5 at 1:100, SIRT6 at 1:500, SIRT7 at 1:100, HKII at 1:100, GLUT1 at 1:1000, SDHA at 1:50, firefly luciferase at 1:500. Post primary antibody incubation, the tissues were washed with blocking buffer twice at an interval of 30 min and were then incubated with Alexa Fluor® 488 or Alexa Fluor® 555 conjugated secondary antibody solution (1:200 dilution) in the humidifying chamber at

room temperature for 1 h in dark. The slides were then washed thrice with 1X PBS followed by addition of DAPI and kept for 5 min at room temperature. The slides were finally washed with 1X PBS 6 times and mounted on a glass slide using mounting media prepared with 0.5% (w/v) n-propylgallate; 20 mM Tris; 70% glycerol at pH = 8.0. The fluorescence images were taken using the Olympus Fluoview FV3000 confocal microscope. The confocal images were taken at 359/461 nm for DAPI, 499/520 nm for Alexa488, and 553/568 nm for Alexa555. The sampling speed for every image was kept as 8.0 μs/pixel (0.56 min per image). Further, all images were quantified using the imageJ software. For the single stained images (i.e., primary tumor tissue sections), the relative expression of the respective protein of interest was quantified with respect to the intensity of the nuclei followed by performing the ordinary one-way analysis of variance (ANOVA) statistical test to determine the statistical significance between the groups (saline, cisplatin, and polytherapy). For all the images with dual staining, we determine the mean intensity of the protein of interest in luciferase positive cells with respect to the number of nuclei for secondary tumor tissue, whereas we determine the mean intensity of ZO-1 in CD31 positive cells with respect to nuclei in the brain sections for understanding the BBB integrity. Statistical significance was measured using ordinary one-way ANOVA and unpaired t-test, respectively.

Dual staining image quantification: For quantification analysis of the dual stained images, we used the ImageJ 1.53t software. The raw data file is opened in the software followed by z-stacking of the images at maximum intensity. After creating a z-stacked image, the image is split into the respective blue (nuclei), green, red, and differential interference contrast (DIC) channels. Initial steps of quantification need only green and red channels to be open (Step 1) which were then merged using merge channel option (Step 2). We then followed the steps given below to quantify the protein of interest (red channel) in cells that are positive for green channel. Briefly, the merged (green and red) image was converted to RGB type and color threshold was selected from Image option (Step 3). Selecting color threshold initially marks all regions (shown by red coloration in step 3 image below) on the image that we would be able to measure for mean intensities. Further, we only select the yellow region from the color threshold spectrum (Step 4) to measure the mean intensity of red in green (Step 5). Finally, to quantify the mean intensity

of red in green with respect to the number of nuclei, we count the number of cells in the image using the Cell Counter plugin in ImageJ (Step 6). Results were plotted as mean intensity of red in green positive cells with respect to number of nuclei. Below we have used an image as an example to show the method of quantification used.

Step1: Splitting green and red channels

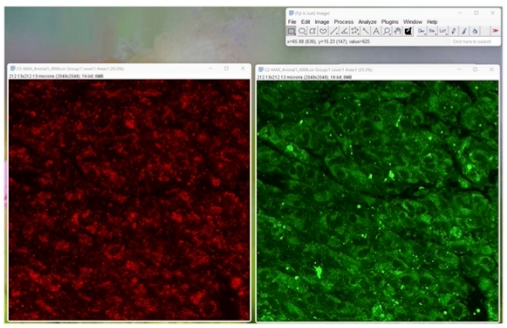

Step2: Merged green and red channels

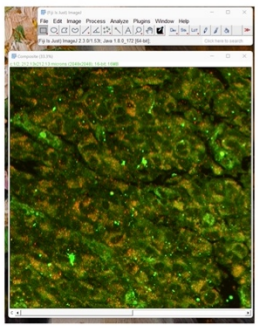

Step3: RGB conversion and color threshold selection

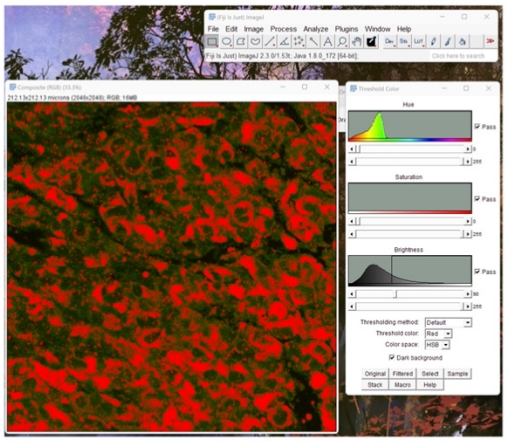

Step4: Color threshold selection of red intensity in green channel by selecting only the yellow region

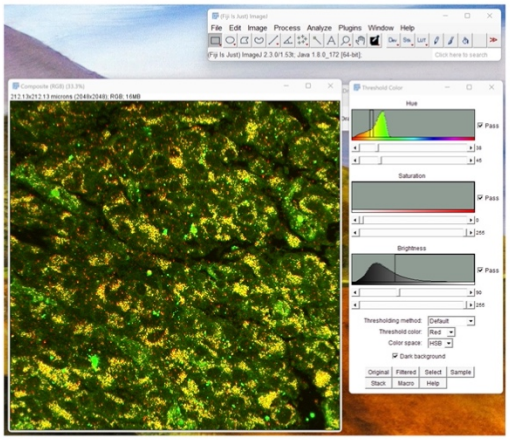

Step5: Mean intensity of red in green measured

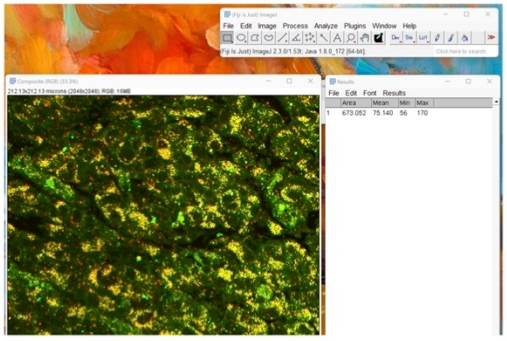

Step6: Number of nuclei counted using cell counter plugin in ImageJ

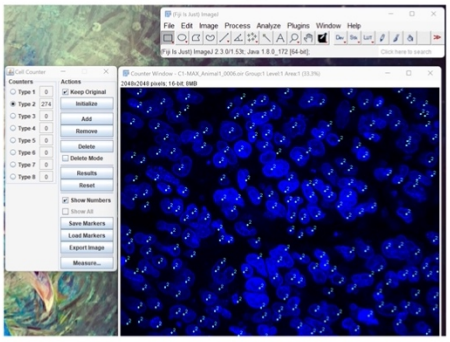

Steps showing the quantification method for dual stained images. All quantifications were performed in ImageJ software.

Behavioral Analyses of BALB/c Albino Mice After Treatment with T-NPs: The behavioral study was performed in N = 15 BALB/c (6 Male and 9 Female) albino mice. Since in this study, we are analyzing toxicity of the T-NP, the delivery vehicle, we used both male and female mice so that the platform can be used for other types of cancers such as lung cancer which also spread to the brain. The mice were randomly divided into three groups with n = 5 (2 male and 3 female) mice per group. The mice in group 1 were administered 100 μL saline. In group 2, the mice were injected with cisplatin at a dosage of 5 mg/kg per dose, biweekly for 4 weeks. In group 3, the mice were injected with the empty brain targeted nanoparticle scaffold, PLGA-*b*-PEG-TPP-NPs (T-NPs) at a dosage of 300 mg/kg per dose, biweekly for 4 weeks. The cumulative dosage for the T-NPs was 2400 mg/kg. All the test articles were injected *via* tail i.v. route. The mice were regularly administered with the test articles following the treatment regimen. To evaluate the effect of T-NPs on the neurocognitive parameters of the mice, we performed open field test, tail suspension test, Y-maze test, and foot placement test.

(1) Open Field Test: The open field test was performed in a Photobeam Activity System which quantifies the number of times the mouse crosses the beam. The path trace of the mouse helps us understand the locomotor cognition of the animals based on the different treatment groups. The mice were individually placed in an open field instrument made from plexiglass. The plexiglass open field instrument was outfitted with photo beam detectors. The detectors are placed under a soft overhead lighting. The activity of each mouse was monitored for 30 min using the Photobeam Activity System software. The apparatus automatically measures the number of beam breaks which is calculated every 5 min. The mice under saline, cisplatin, and T-NPs treatment were tested for having any anxiety-like behavior.

(2) Tail Suspension Test: The tail suspension test was performed in the Med Associates automated testing system. This automated system is comprised of a testing chamber which is open in the front and a vertical metal bar that is attached to a strain gauge. Each mouse is suspended through the vertical metal bar by attaching its tail to the bar. The movement that the mouse makes while being suspended in the chamber is detected by the metal bar and measured by the Med Associates software. The mouse is suspended

for a total time of 6 min and time spent in immobility was calculated during the last 4 min of the test.

(3) Y-maze Test: For performing the Y-maze test, a Y-shaped chamber made up of grey plexiglass was used, where each arm of the chamber represented a specific region/arm for the mouse to be in. This test was used to measure the spatial working memory. The arm facing outward towards the experimenter was named the 'Start' arm. Out of the two distal arms, right arm was termed as the "Familiar' arm, and the left arm was termed as the 'Novel' arm. The novel arm was obstructed using a barrier during the preliminary acquisition phase. The mouse was first allowed to explore the start arm and the familiar arm for 2 min by placing the mouse at the end of the start arm. This was followed by placing the mouse in its cage for an intertrial interval of 30 min. Post the intertrial interval, the mouse was placed at the end of the start arm and allowed to explore all the arms of the Y-maze including the novel arm for 2 min. The measurement of the spatial memory starts from the time the mouse leaves the start arm and explores the novel and the familiar arms. The total time the mouse spends exploring the novel arm compared to the familiar arm signifies whether a mouse is suffering from cognitive impairment. Entry into an arm is considered only when all four paws of the mouse are placed within the arm. Any time during which the mouse is staying stationary or engaging in self-grooming itself was excluded from the calculation.

(4) Foot Placement Test: The walking pattern or gait abnormalities was evaluated by performing the foot placement analysis. The foot placement study was performed using non-toxic grade color of the fore and hind limbs of mice followed by tracing their path and strides across a white membrane. The hind limbs and fore limbs of the mice were dipped in non-toxic watercolor paint. The mice were then allowed to walk on white paper within a narrow plastic corridor. An enclosed safety platform with food was placed at the end of the walkway, which serves as a motivation for the movement of the mice down the corridor. The imprints of the limbs on the paper as the mice traverse the corridor were used to analyze the behavioral outcomes by measuring stride length and stride width. For each animal, the stride length was measured as the distance in millimeters between the hind limbs of the successive foot placements. The stride width was measured as the distance in millimeters between the left and right hind limbs. The data for stride length of

each animal is represented as the mean from a minimum of 3 stride length measurements and the data for stride width is represented as the mean from 4 stride width measurements.

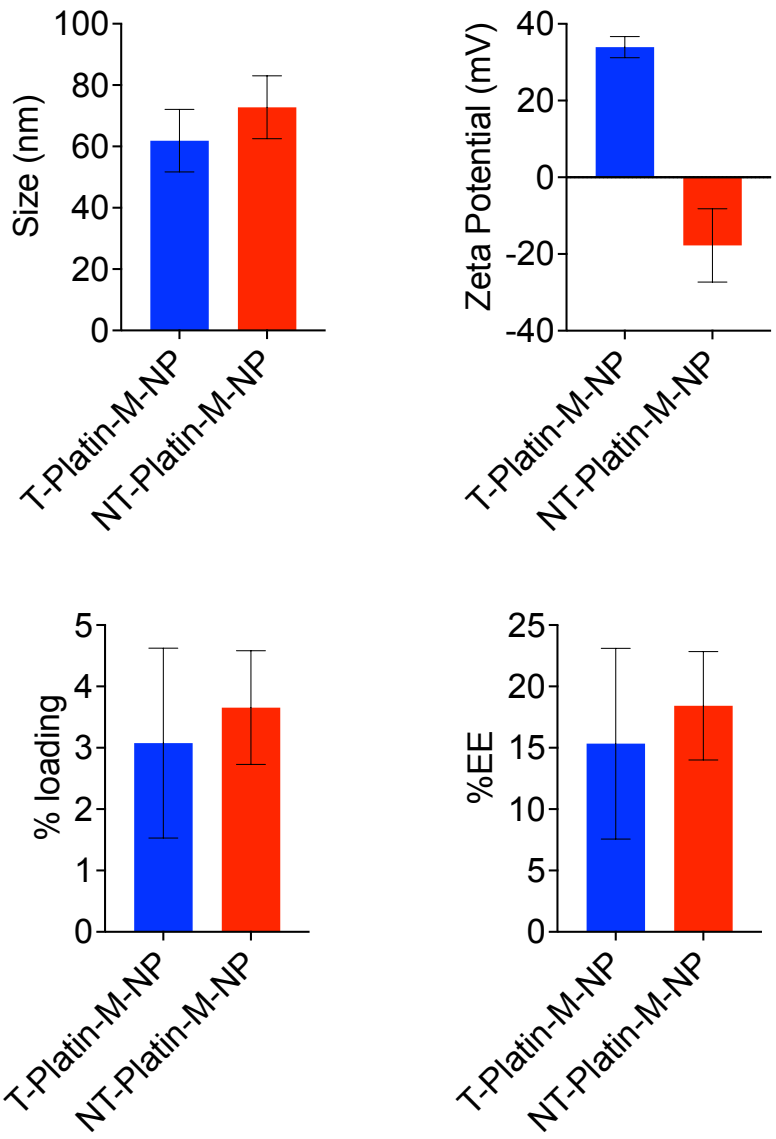

Figure S1. Size ($Z_{average}$), zeta potential, percent loading, and encapsulation efficacy of NT/T-Platin-M-NPs.

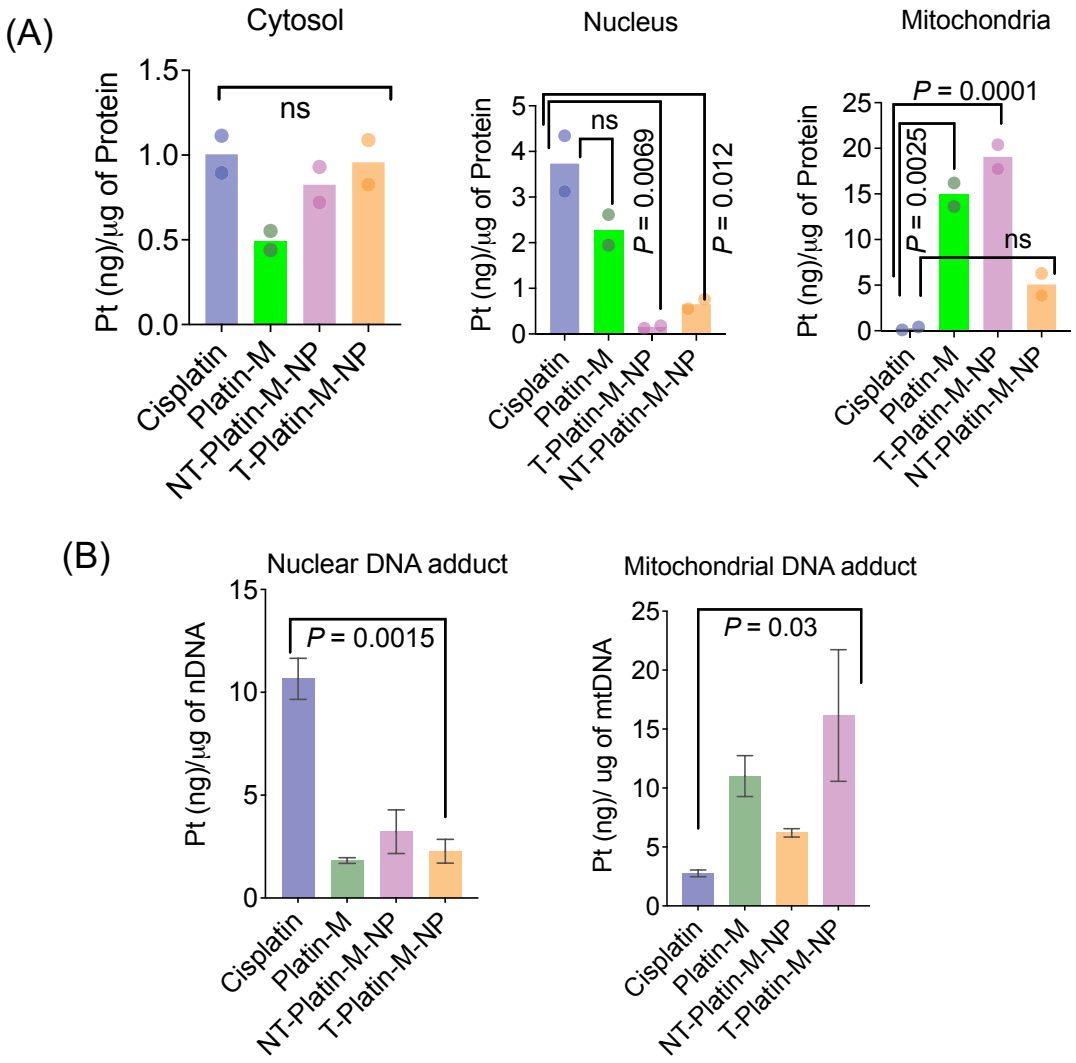

Figure S2. (A) Distribution of cisplatin, Platin-M, NT-Platin-M-NPs, and T-Platin-M-NPs in cytosolic, nuclear, and mitochondrial fractions of MDA-MB-231-BR cells. (B) Comparison of Pt-nDNA and Pt-mtDNA adducts for cisplatin, Platin-M, NT-Platin-M-NP, and T-Platin-M-NPs in MDA-MB-231-BR cells. [Cisplatin]: 10 μM, [Platin-M]: 10 μM, and concentration of T-Platin-M-NP or NT-Platin-M-NP was calculated with respect to [Platin-M]: 10 μM. Statistical analyses were performed using one-way ANOVA with multiple comparison.

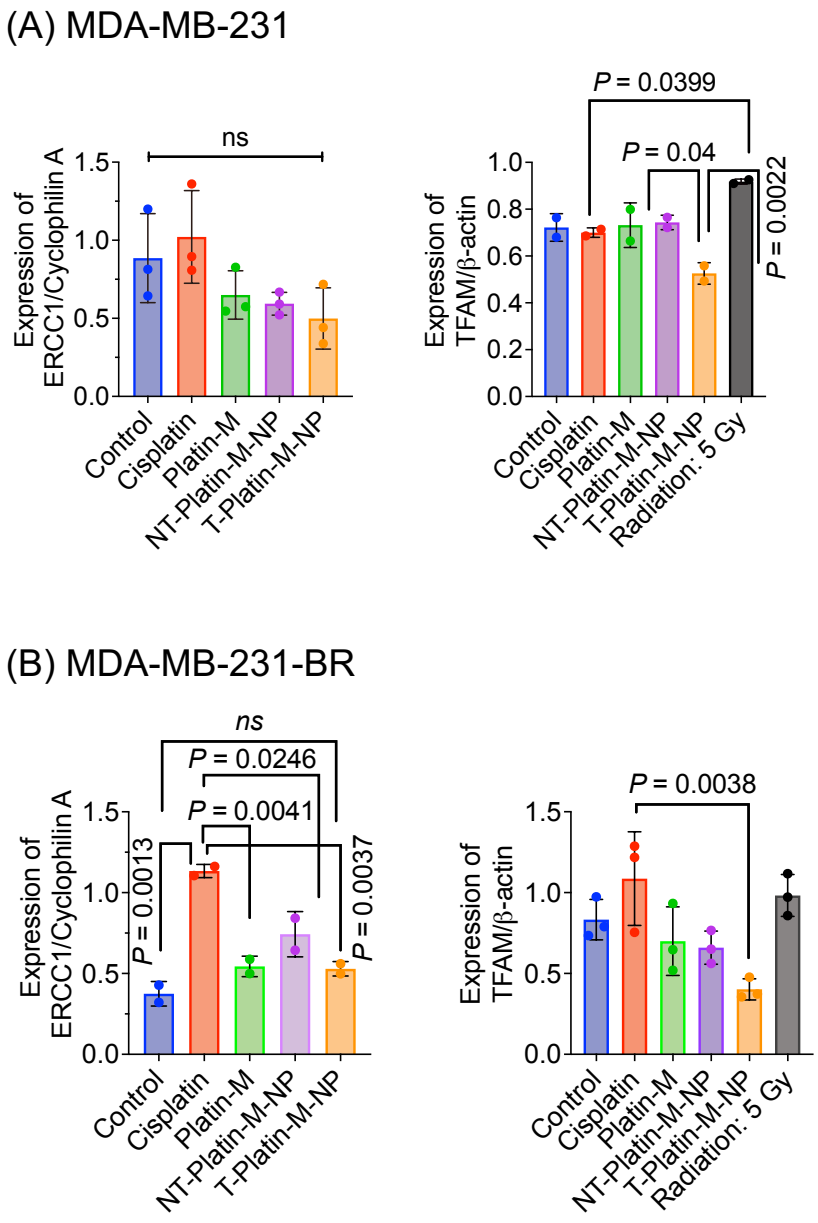

Figure S3. Quantitative analysis from western blot images for expression of ERCC1 and TFAM in (A) MDA-MB-231 and (B) MDA-MB-231-BR cells after treating with cisplatin (10 μM), Platin-M (10 μM), NT-Platin-M-NP, T-Platin-M-NP (10 μM with respect to Platin-M), or upon radiation of 5 Gy. Statistical analyses were performed using ordinary one-way ANOVA with multiple comparison.

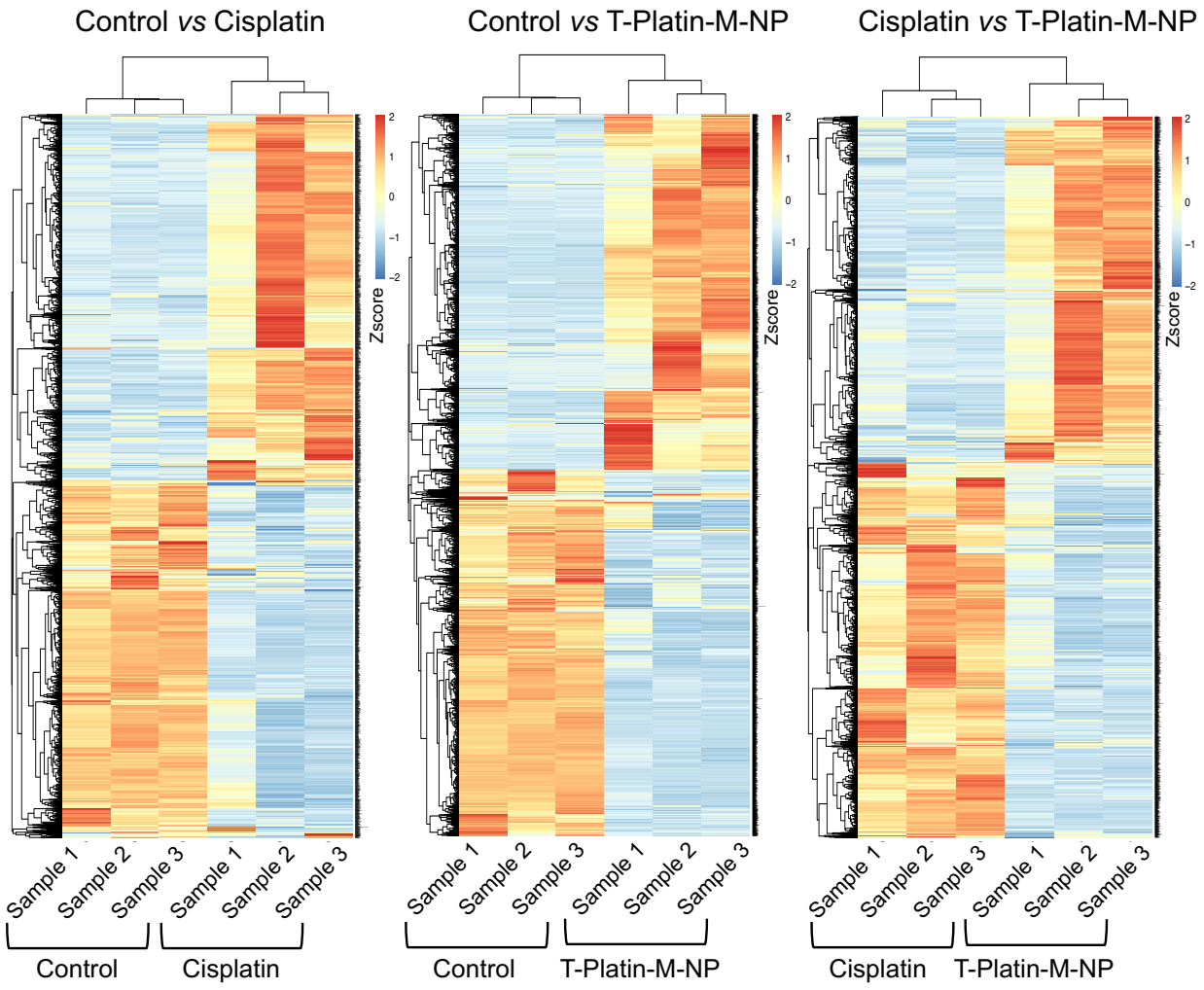

Figure S4. Comparison of whole genome cluster heat map of MDA-MB-231-BR cells treated with cisplatin (10 μM), T-Platin-M-NP (10 μM with respect to Platin-M) and nontreated cells.

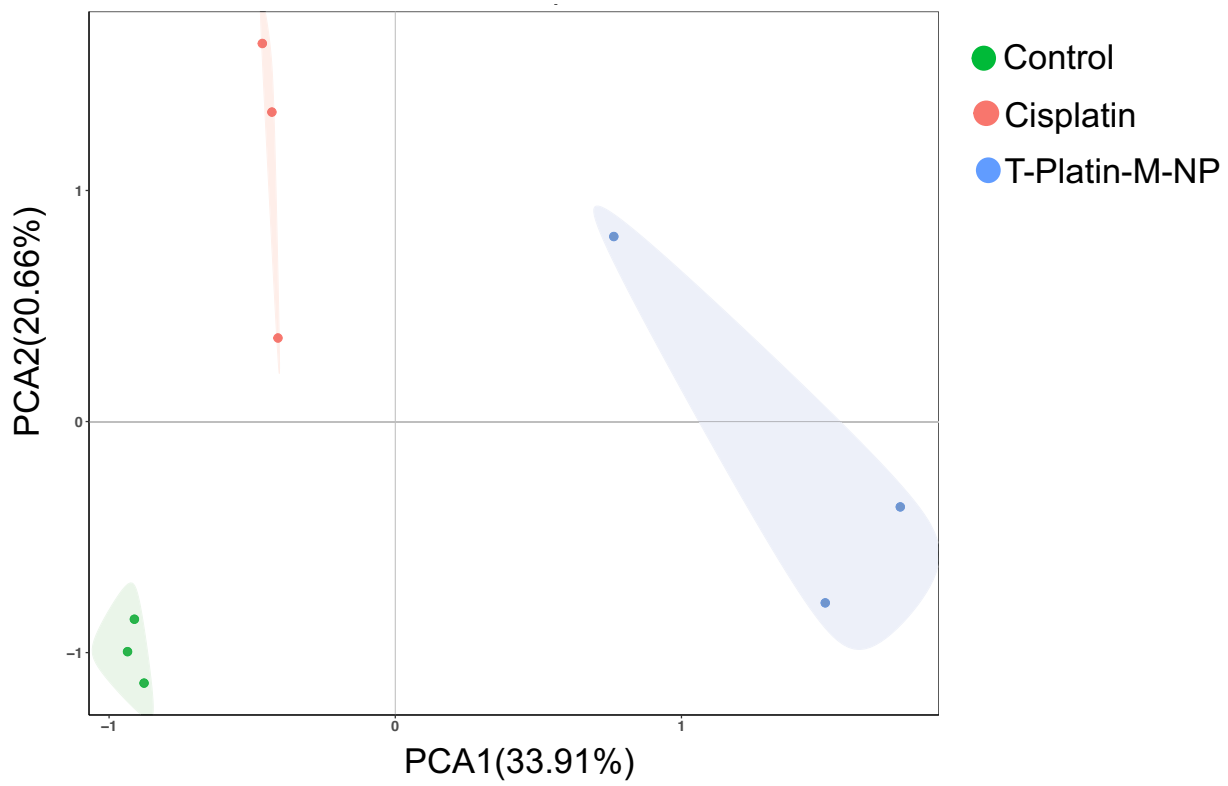

Figure S5. Principal complement analysis (PCA) plot of MDA-MB-231-BR cells treated with cisplatin (10 μM), T-Platin-M-NP (10 μM with respect to Platin-M) and nontreated cells.

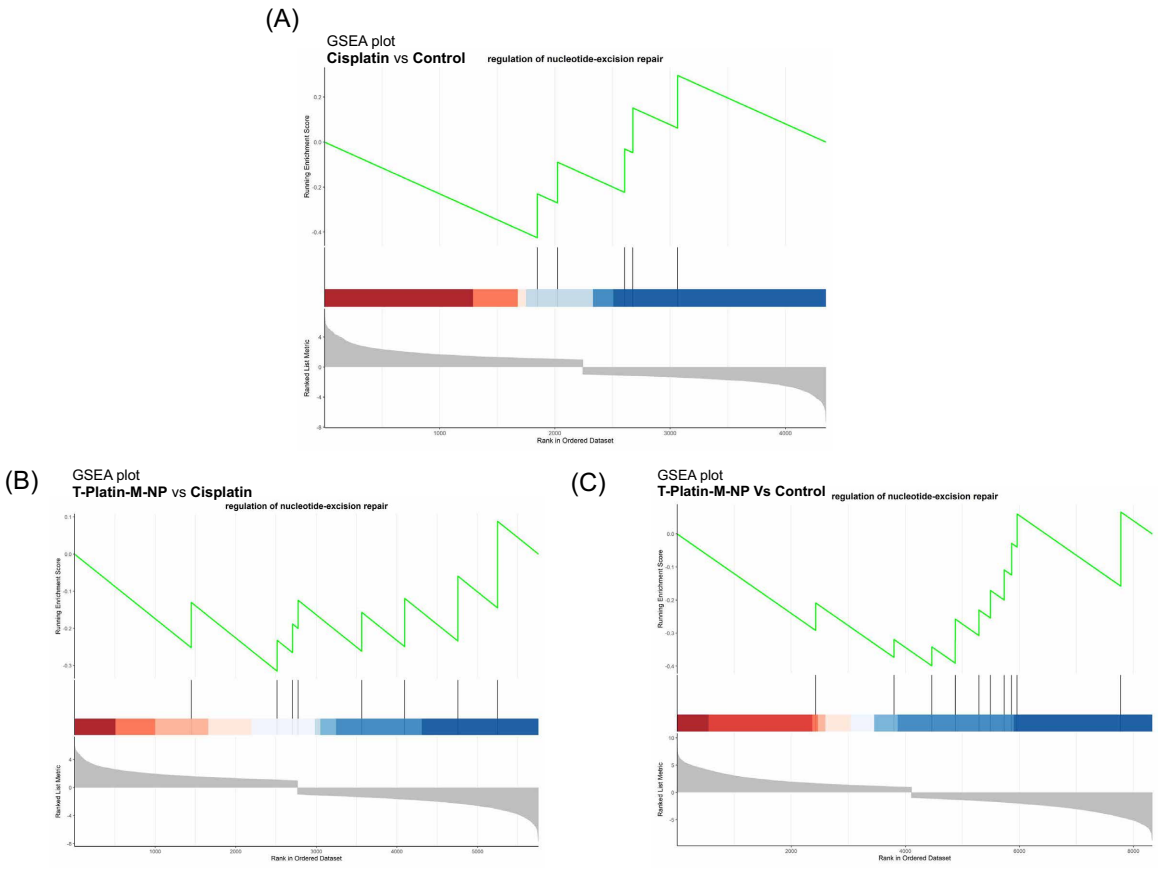

Fig. S6. Gene set enrichment analysis (GSEA)-enrichment plots of representative gene sets from KEGG:NER pathway. GSEA plot for NER pathway between (A) Cisplatin vs Control, (B) T-Platin-M-NP vs Cisplatin, (C) T-Platin-M-NP vs control.

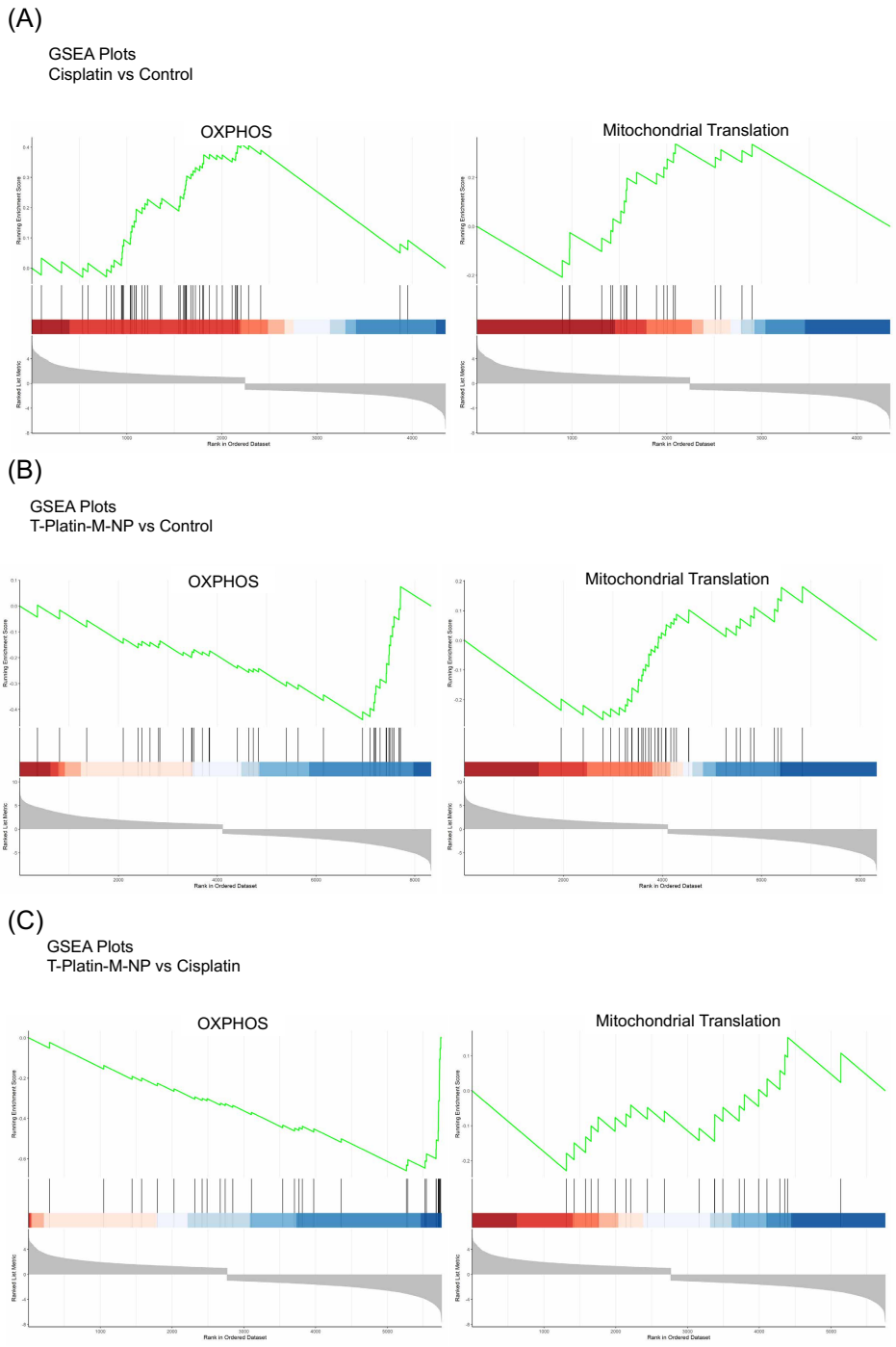

Fig. S7. Gene set enrichment analysis (GSEA)-enrichment plots of representative gene sets from KEGG:NER pathway. GSEA plots for OXPHOS and mitochondrial translation pathways between (A) Cisplatin vs Control, (B) T-Platin-M-NP vs control, (C) T-Platin-M-NP vs cisplatin.

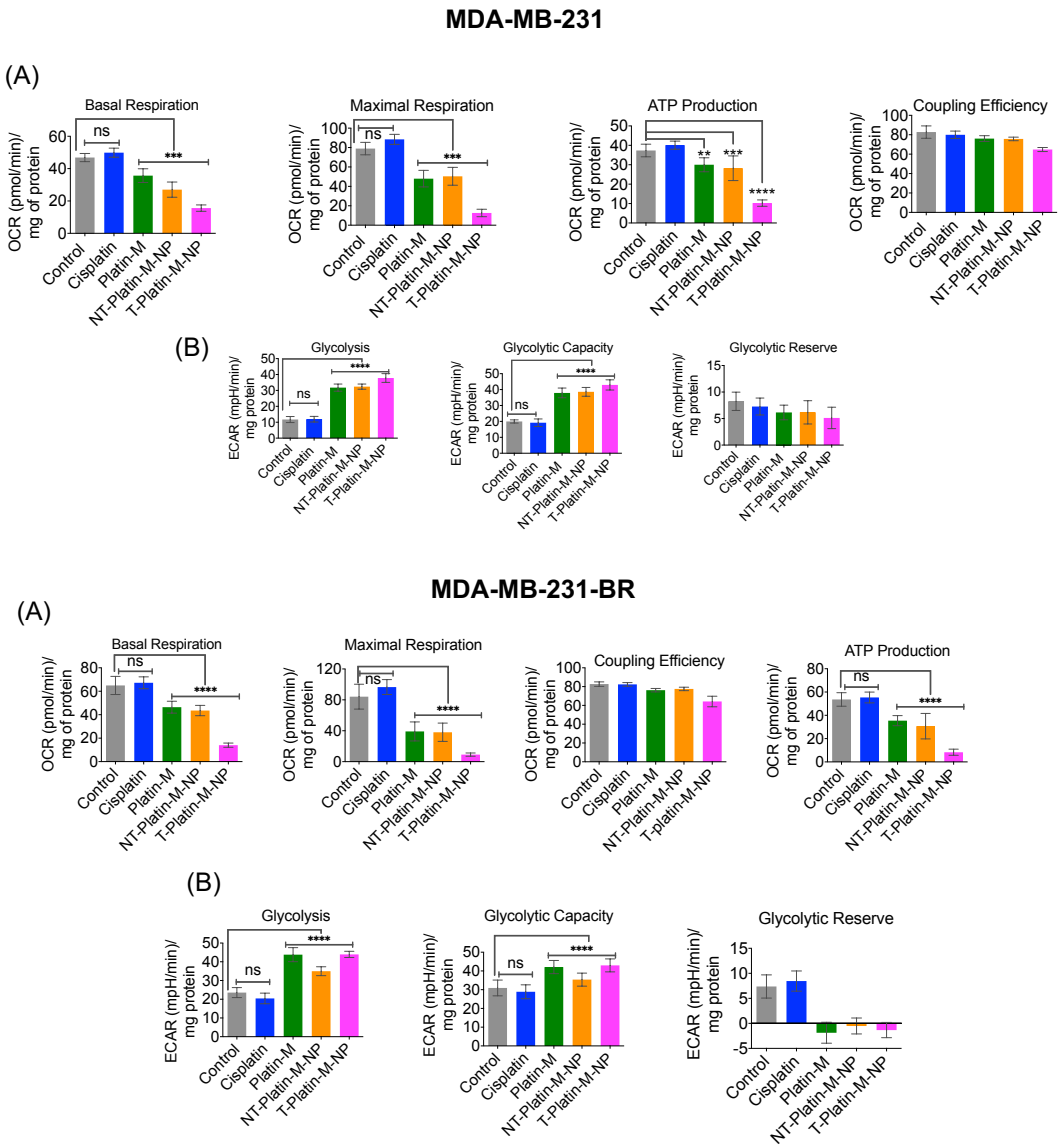

Figure S8. (A) Mitochondrial basal respiration, maximal respiration, ATP production, coupling efficiency and (B) glycolysis, glycolytic capacity and glycolytic reserve of MDA-MB-231 cells and MDA-MB-231-BR cells upon treatment with cisplatin, Platin-M, NT-Platin-M-NP, T-Platin-M-NP for 12 h. [Cisplatin]: 10 μM, [Platin-M]: 10 μM, and concentration of T-Platin-M-NP or NT-Platin-M-NP was calculated with respect to [Platin-M]: 10 μM. Mitostress assay was run using oligomycin (1 μM), FCCP (1 μM), and a mixture of antimycin-A and rotenone (1 μM each) in ports A, B, and C respectively using Seahorse XF^{e}96 Extracellular Flux Analyzer. Statistical analyses were performed using ordinary one-way ANOVA with multiple comparison.

(A) MDA-MB-231

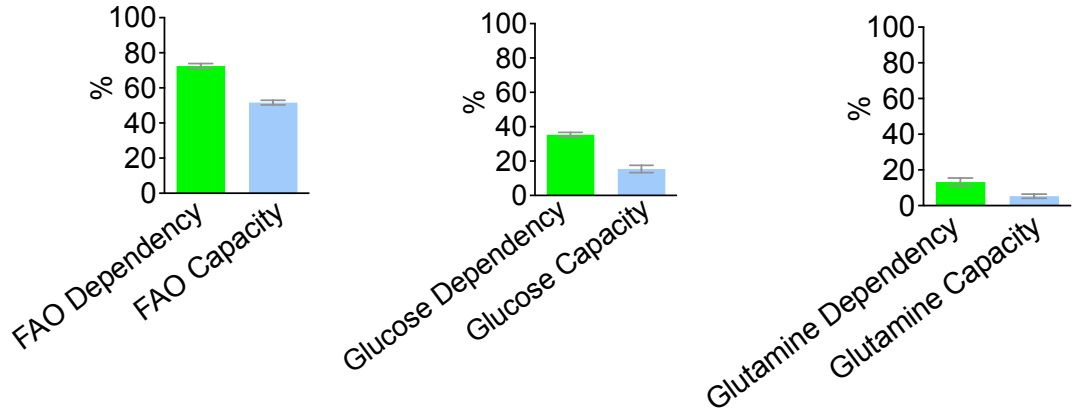

(B) MDA-MB-231-BR

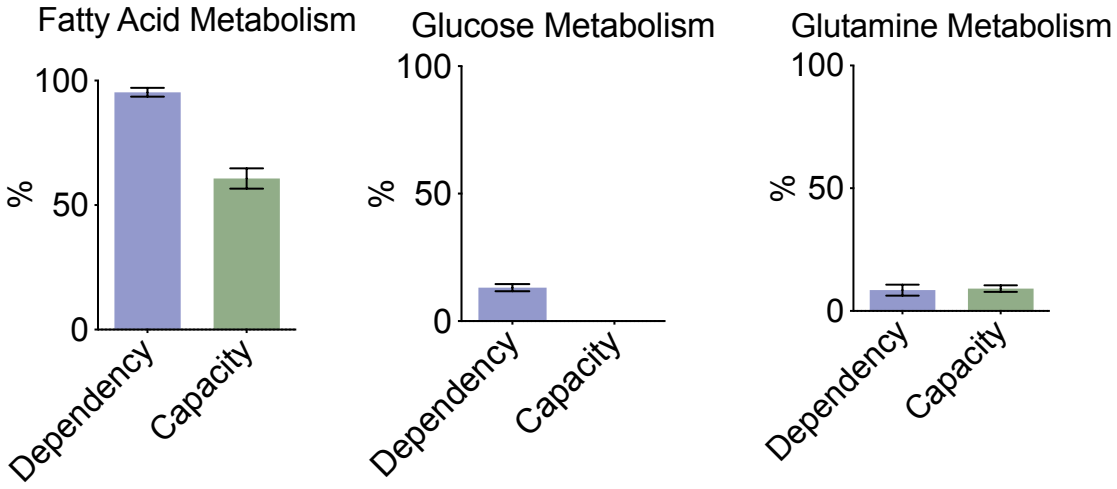

Figure S9. Fatty acid metabolism, glucose metabolism, glutamine metabolism of (A) MDA-MB-231 cells and (B) MDA-MB-231-BR cells. Etomoxir, UK5099 and BPTES concentration were constant at 4 μM, 2 μM, and 3 μM, respectively for the fuel flex assay.

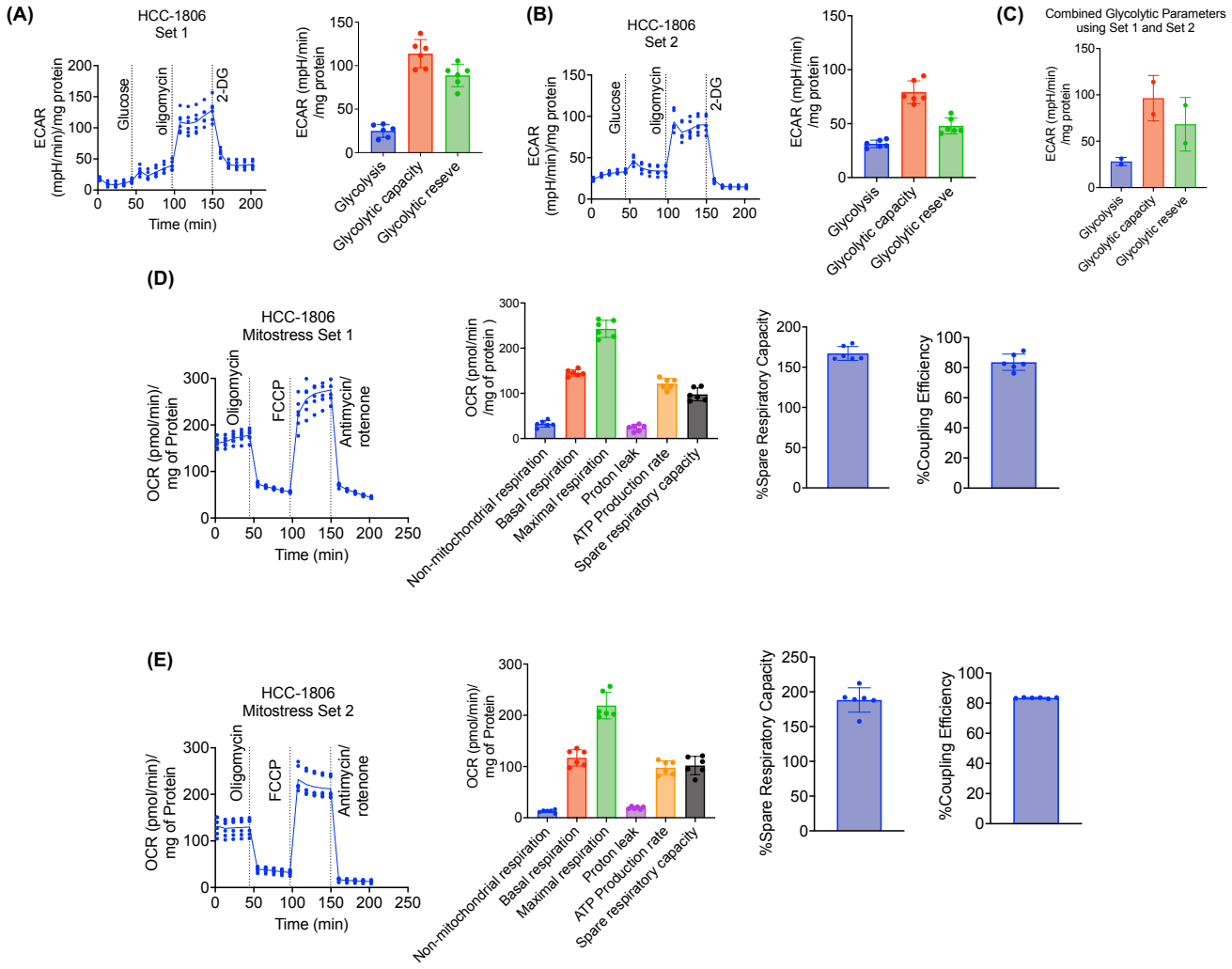

Figure S10. (A-C) Glycolysis, glycolytic capacity, and glycolytic reserve; (D-E) mitochondrial OXPHOS, basal respiration, maximal respiration, proton leak, ATP production, spare respiratory capacity, percent spare respiratory capacity, and percent coupling efficiency of TNBC HCC1806 cell line. Mitostress assay was run using oligomycin (1 μM), FCCP (1 μM), and a mixture of antimycin-A/rotenone (1 μM) each in ports A, B, and C respectively using Seahorse XF^{e}96 Extracellular Flux Analyzer. Glycolytic stress test was run using glucose: 10 mM, oligomycin: 1 μM, and 2-Deoxyglucose (2-DG): 50 mM in ports A, B, and C, respectively using Seahorse XF^{e}96 Extracellular Flux Analyzer.

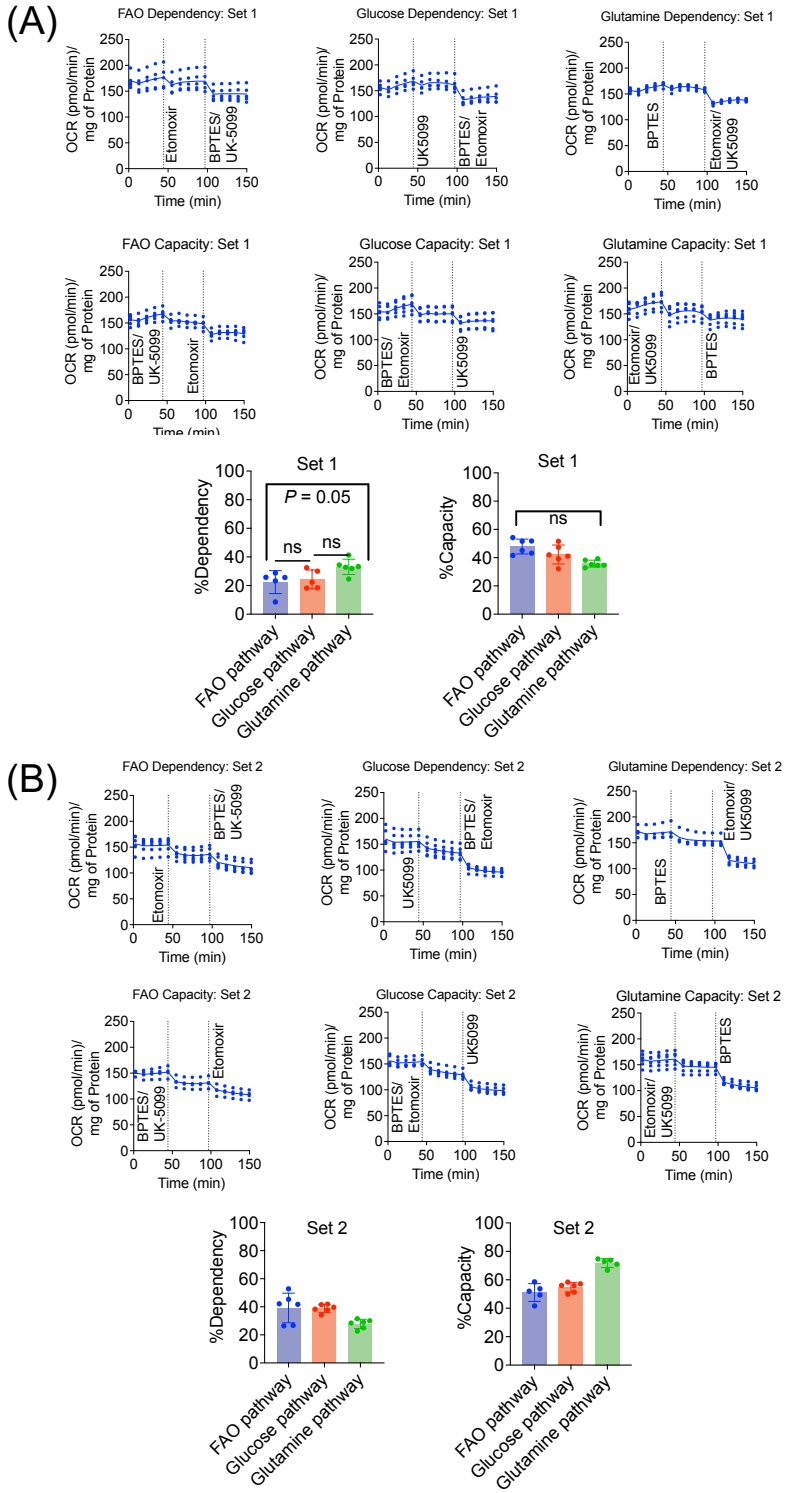

Figure S11. Fatty acid metabolism, glucose metabolism, glutamine metabolism of HCC1806 cell line.

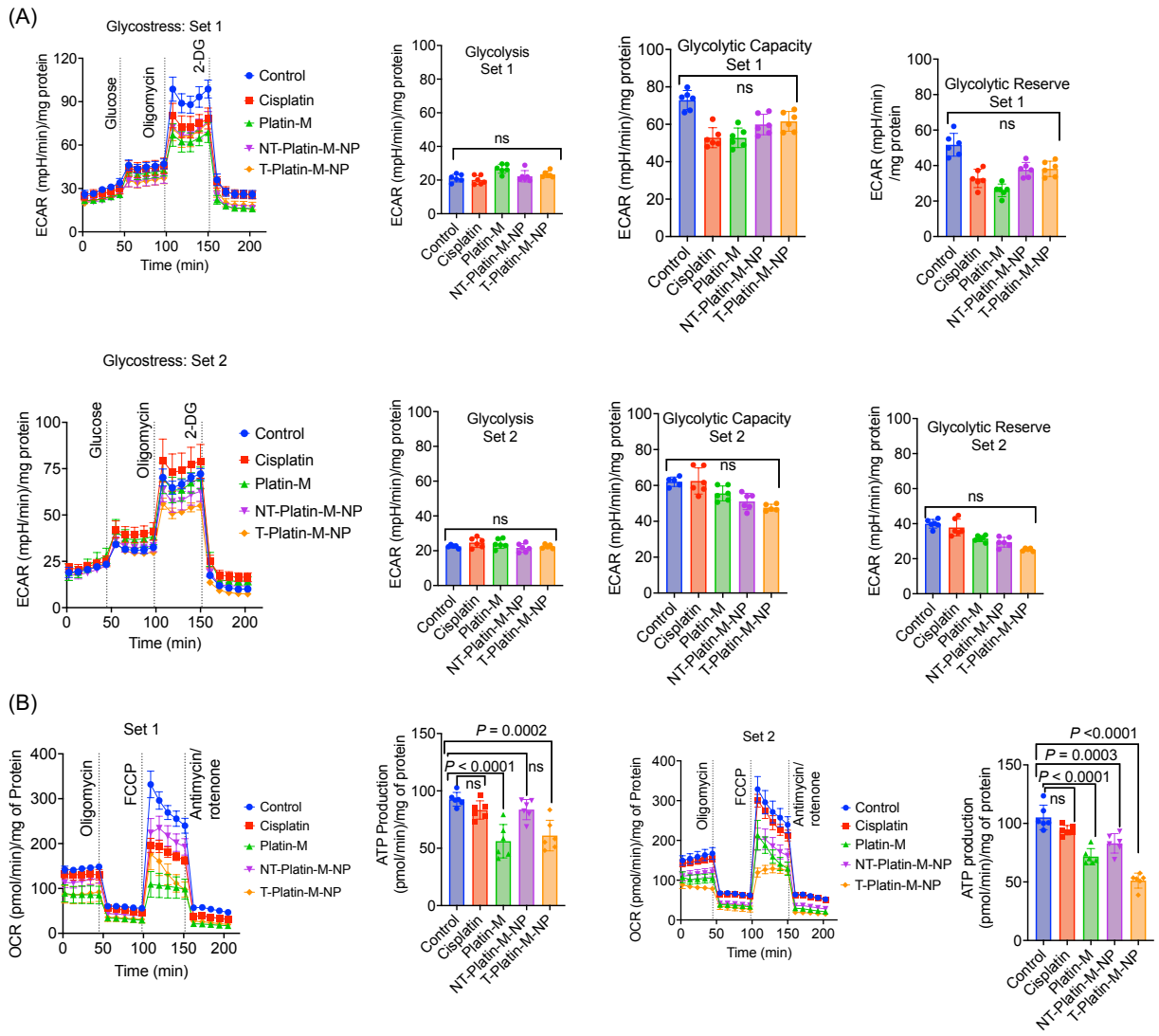

Figure S12. Effects on (A) glycolysis, glycolytic capacity and glycolytic reserve and (B) mitochondrial OXPHOS and ATP production of HCC1806 cells upon treatment with cisplatin, Platin-M, NT-Platin-M-NP, T-Platin-M-NP for 12 h. [Cisplatin]: 10 μM, [Platin-M]: 10 μM, and concentration of T-Platin-M-NP or NT-Platin-M-NP was calculated with respect to [Platin-M]: 10 μM. Glycolytic stress test was run using glucose: 10 mM, oligomycin: 1 μM, and 2-Deoxyglucose (2-DG): 50 mM in ports A, B, and C, respectively using Seahorse XF^{e}96 Extracellular Flux Analyzer. Mitostress assay was conducted using oligomycin (1 μM), FCCP (1 μM), and a mixture of antimycin-A/rotenone (1 μM) each in ports A, B, and C respectively using Seahorse XF^{e}96 Extracellular Flux Analyzer. Statistical analyses were performed using ordinary one-way ANOVA with multiple comparison.

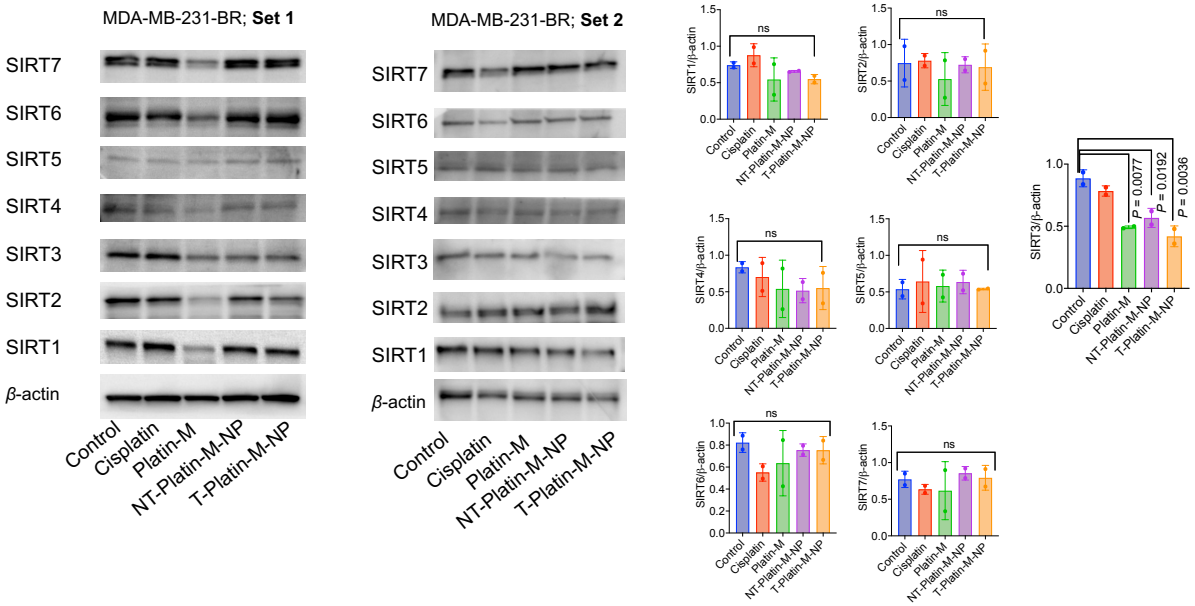

Figure S13. Effect of Platin-M and its NPs on SIRT1-7 using Western blot analyses for expression of SIRT1-7 in MDA-MB-231-BR cells after treating with cisplatin (10 μM), Platin-M (10 μM), NT-Platin-M-NP, and T-Platin-M-NP (10 μM with respect to Platin-M) for 24 h. Statistical analyses were performed using ordinary one-way ANOVA with multiple comparison.

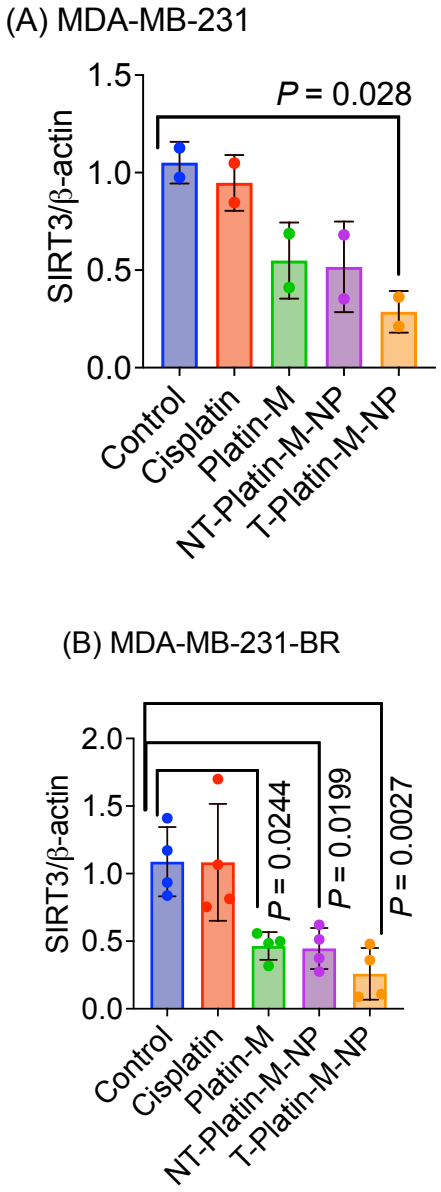

Figure S14. Quantitative analysis from western blot images for expression of SIRT3 in (A) MDA-MB-231 (Data using two independent sets of experiments) and (B) MDA-MB-231-BR cells (Data using four independent experimental sets) after treating with cisplatin (10 μM), Platin-M (10 μM), NT-Platin-M-NP, and T-Platin-M-NP (10 μM with respect to Platin-M). Statistical analyses were performed using ordinary one-way ANOVA with multiple comparison.

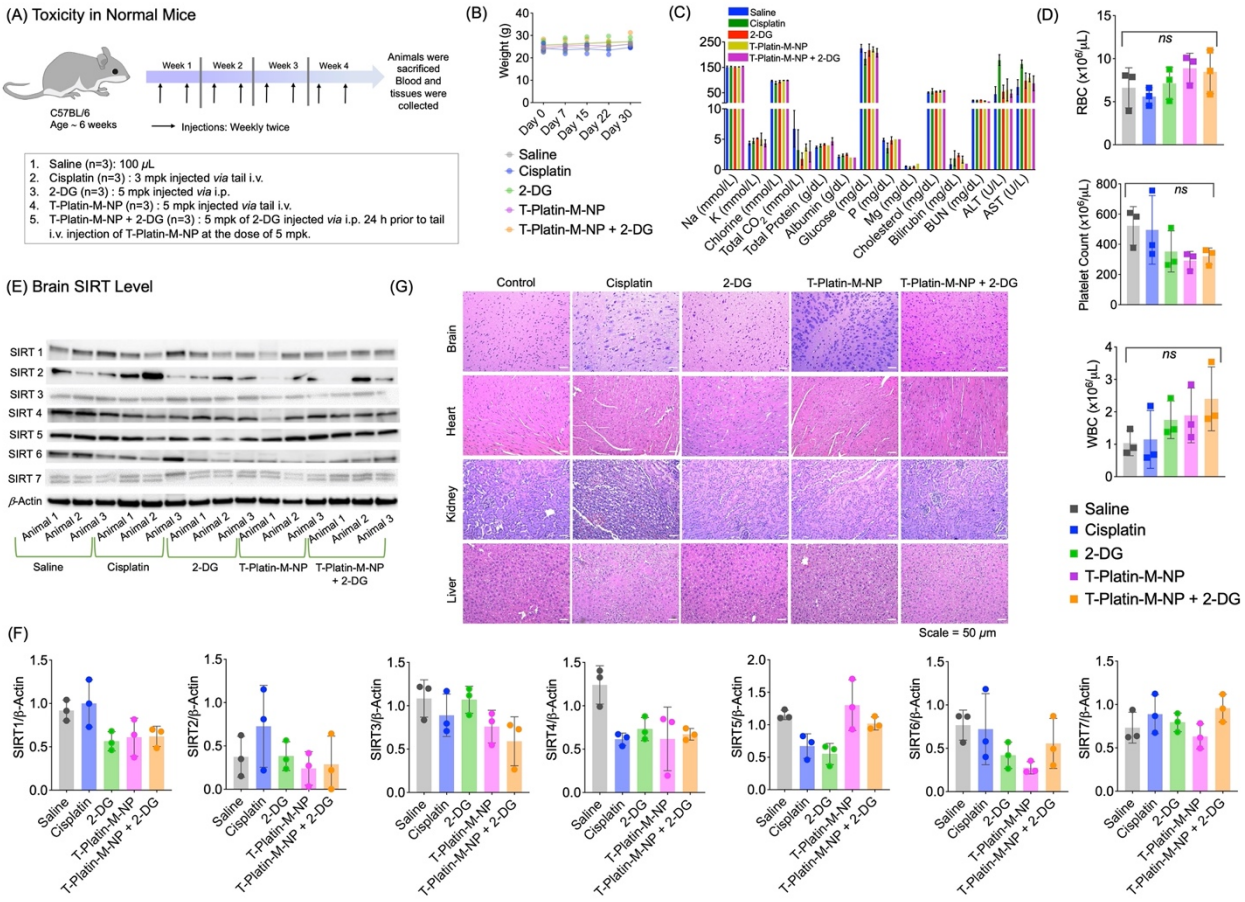

Figure S15. Toxicity of multi-dose T-Platin-M-NP alone or in combination with 2-DG in normal mice. (A) Timeline showing biweekly injections and dosages of cisplatin, 2-DG, T-Platin-M-NP, and T-Platin-M-NP + 2-DG in C57BL/6 mice with n = 3 animals per group. Cumulative dose over 4 weeks: cisplatin, 24 mg/kg; 2-DG, 40 mg/kg; T-Platin-M-NP, 40 mg/kg. (B) Changes in body weight of the treated animals over the course of one month. (C) Measurements of various ions, serum proteins, cholesterol, and liver enzymes and (D) blood cell count in the blood of treated mice as indicators of toxicity. (E) Western Blot and (F) the corresponding quantifications showing levels of SIRT 1-7 in the brains of the treated mice. (G) H & E images of the organs related to our study. Scale bar 50 μm.

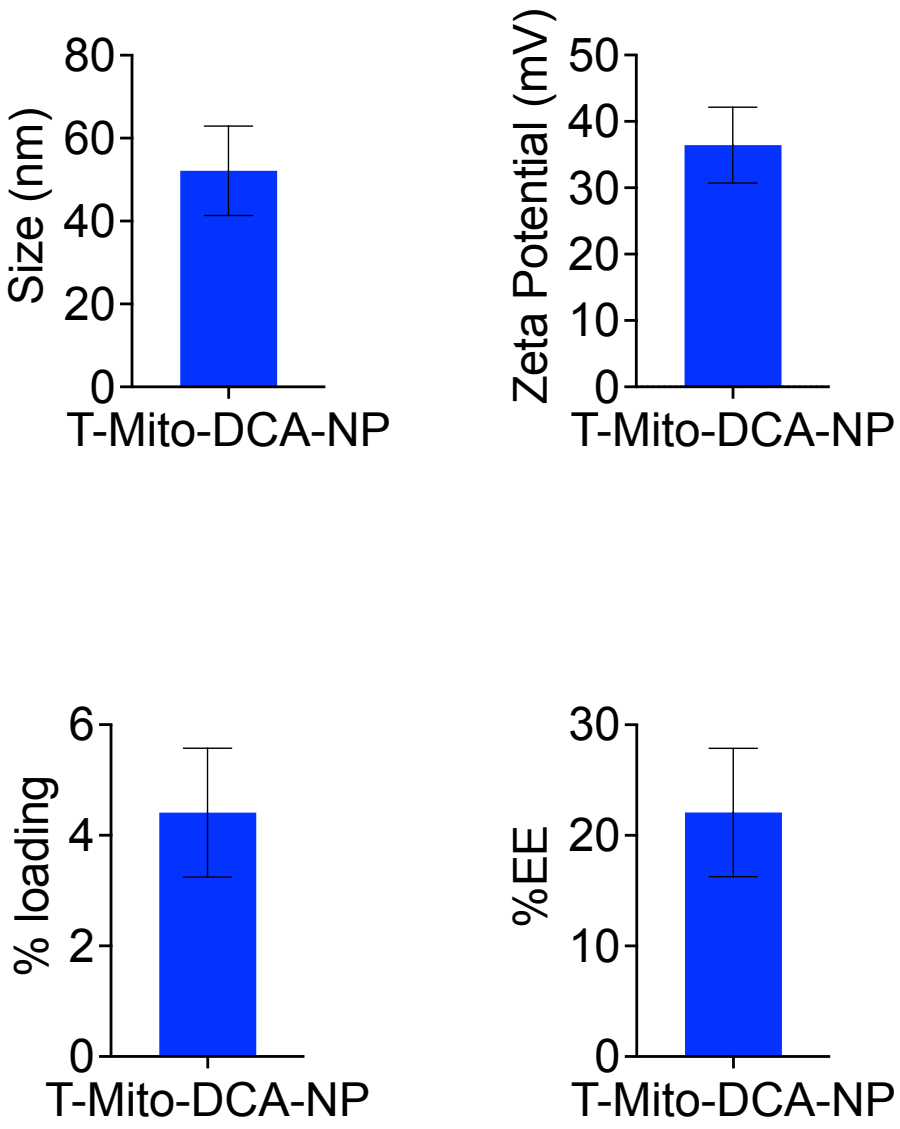

Figure S16. Size, zeta potential, percent Mito-DCA loading, and encapsulation efficacy of T-Mito-DCA-NP measured using DLS and HPLC.

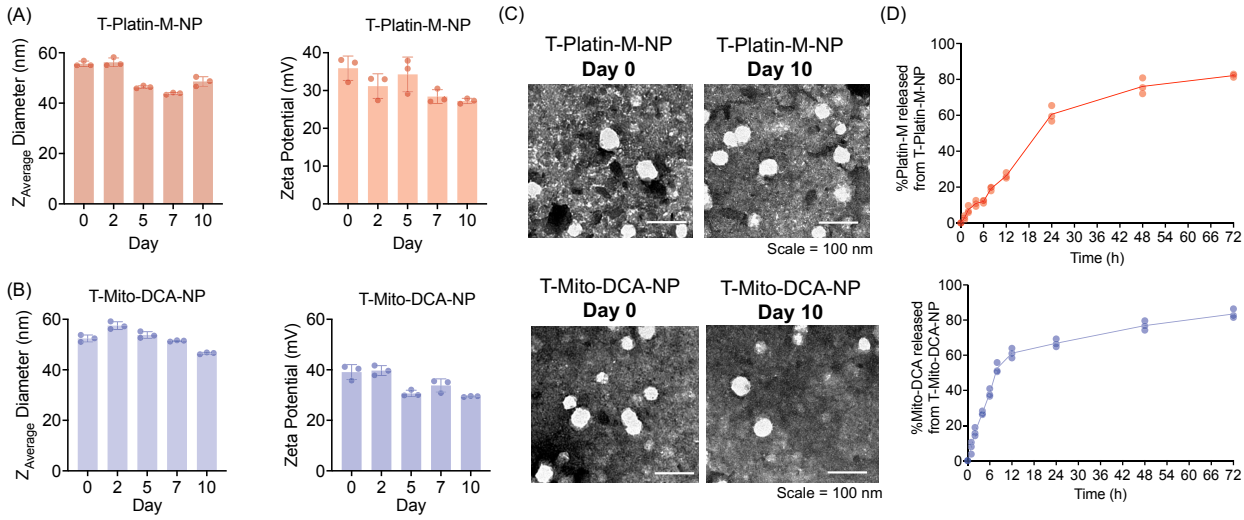

Figure S17. Stability of nanoparticles and release kinetics of the payloads. Stability of (A) T-Platin-M-NPs and (B) T-Mito-DCA-NPs as determined by hydrodynamic diameter and zeta potential measurements after storing at 4 °C over a period of 10 days. (C) TEM images of T-Platin-M-NP and T-Mito-DCA-NP on the day of preparation and after 10 days of storage at 4 °C. (D) Release kinetics study of Platin-M from T-Platin-M-NPs measured by ICP-MS and release kinetics study of Mito-DCA from T-Mito-DCA-NPs measured using HPLC. The mobile phase in HPLC for Mito-DCA detection was 3% acetonitrile in water to 100% acetonitrile for 20 mins followed 100% acetonitrile for 10 min. The peak corresponds to Mito-DCA was observed at 25.7 min (between 25.5 -26.5 min) at 284 nm.

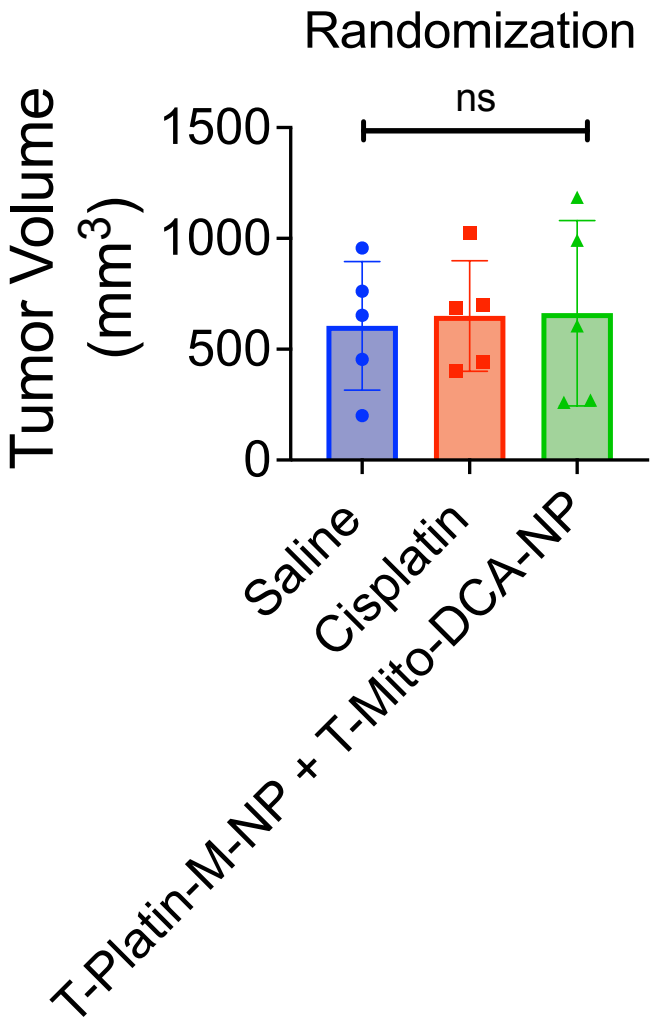

Figure S18. Data illustrating the randomization of animals based on primary tumor volume to further perform the biodistribution analysis.

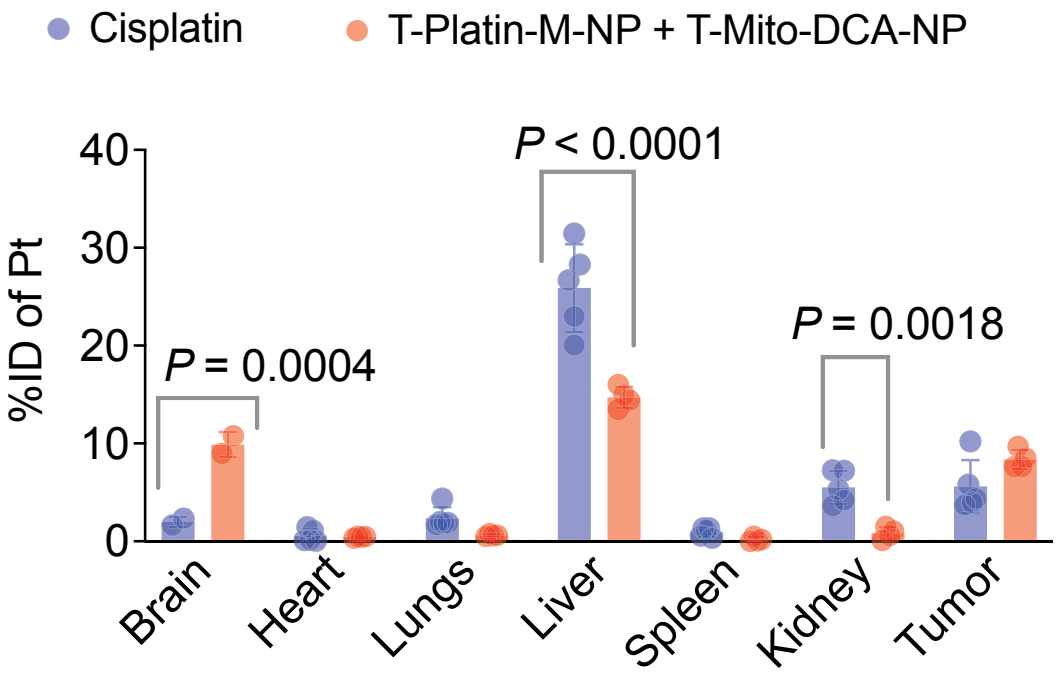

Figure S19. Biodistribution of %injected dose of Pt in cisplatin and T-Platin-M-NP+ T-Mito-DCA-NP in various organs of BALB/c nude mice *via* ICP-MS. All statistical analyses were performed using 2way ANOVA with multiple comparisons.

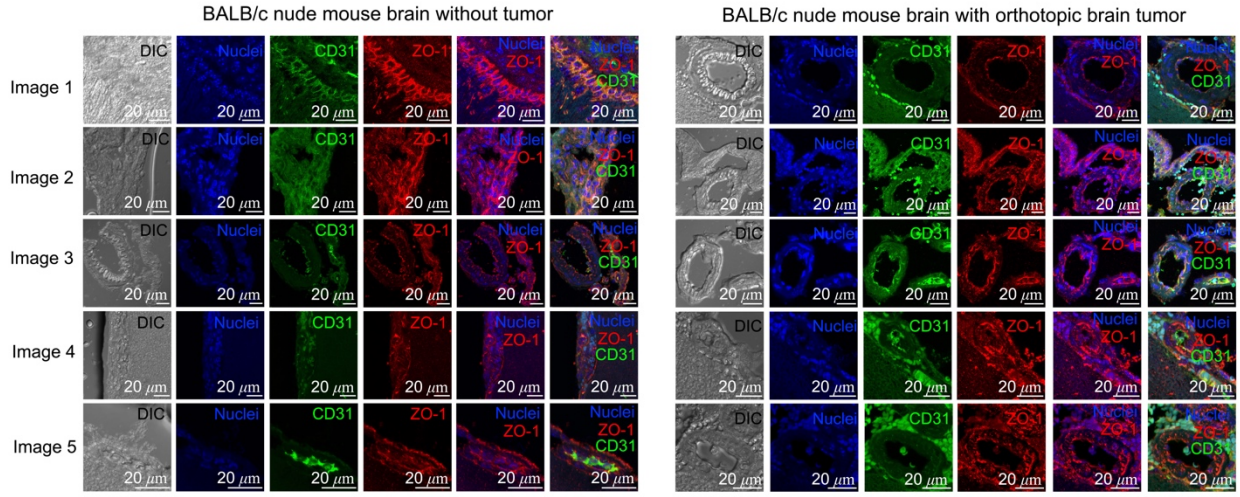

Figure S20. Immunofluorescence images depicting the blood brain barrier (BBB) integrity by observing and quantifying the ZO-1 intensity in endothelial cells in coronal brain sections between BALB/c nude mice without any tumor implantation and BALB/c nude mice with orthotopic brain tumor *via* intracranial stereotactic tumor implantation. Nuclei were stained with DAPI, endothelial cells were stained with CD31, and tight-junction protein ZO-1 was used to analyze the BBB integrity.

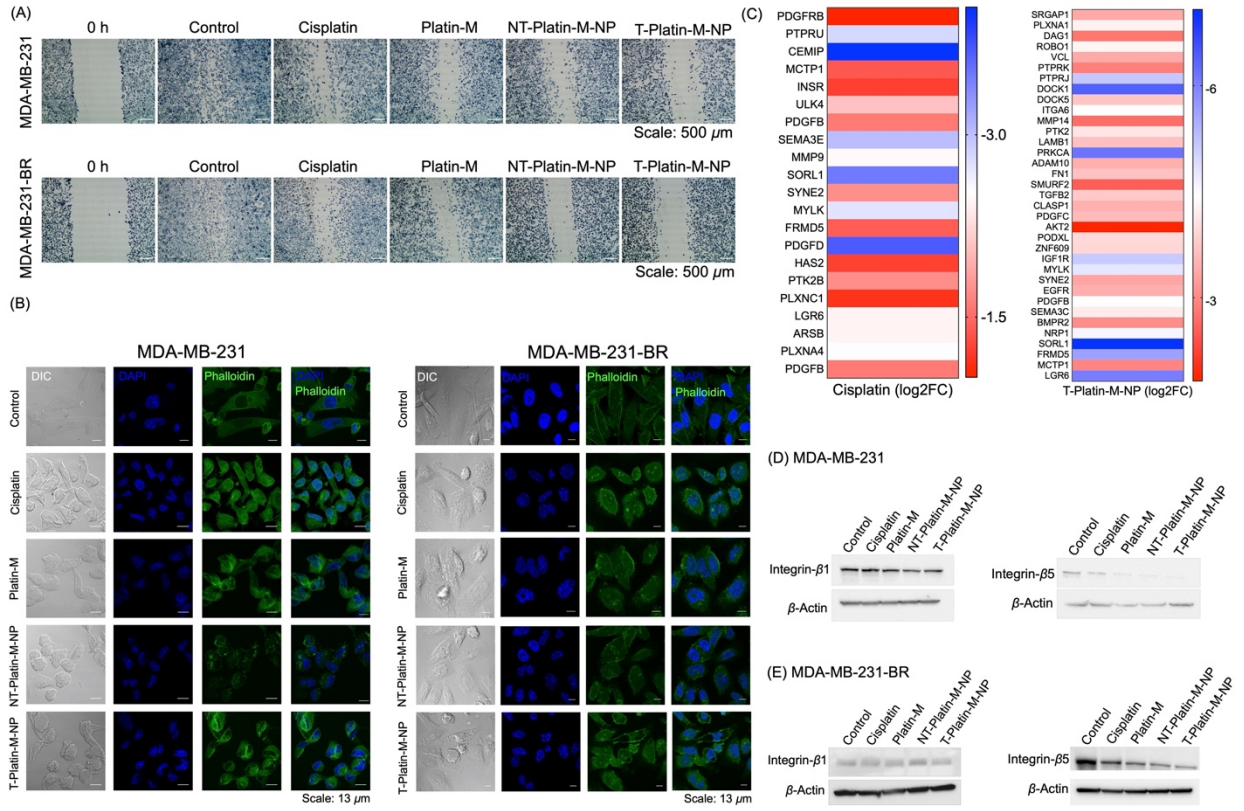

Figure S21. T-Platin-M-NPs Inhibits Cellular Migration and Disrupts Actin Organization. (A) Brightfield microscopy images showing the effect of T-Platin-M-NPs in inhibiting the cellular migration in MDA-MB-231 and MDA-MB-231-BR cells. (B) Immunofluorescence images showing the phalloidin staining to visualize the disruption in actin organization upon treatment with test articles. Scale bar: 13 μm. (C) Heatmap showing the downregulation of genes involved in cellular migration in cisplatin and T-Platin-M-NPs treated MDA-MB-231-BR cells with respect to log2 fold change. Western Blot analyses in (D) MDA-MB-231 and (E) and MDA-MB-231-BR cells showing the change in expression of Integrin-β1 and Integrin-β5.

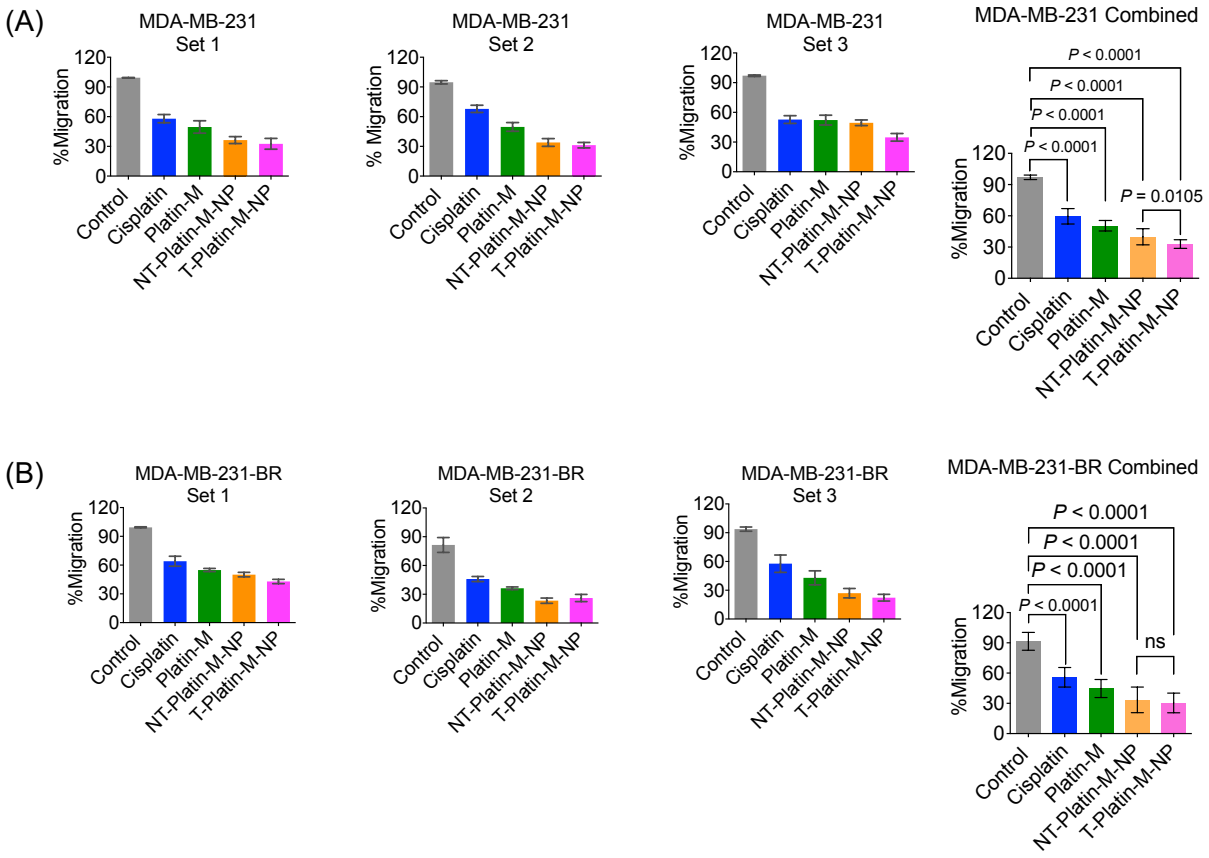

Figure S22. Effect of test articles on cellular migration of (A) MDA-MB-231 and (B) MDA-MB-231-BR cells. [Cisplatin]: 10 μM, [Platin-M]: 10 μM, and concentration of T-Platin-M-NP or NT-Platin-M-NP was calculated with respect to [Platin-M]: 10 μM. Statistical analyses were performed using ordinary one-way ANOVA with multiple comparison.

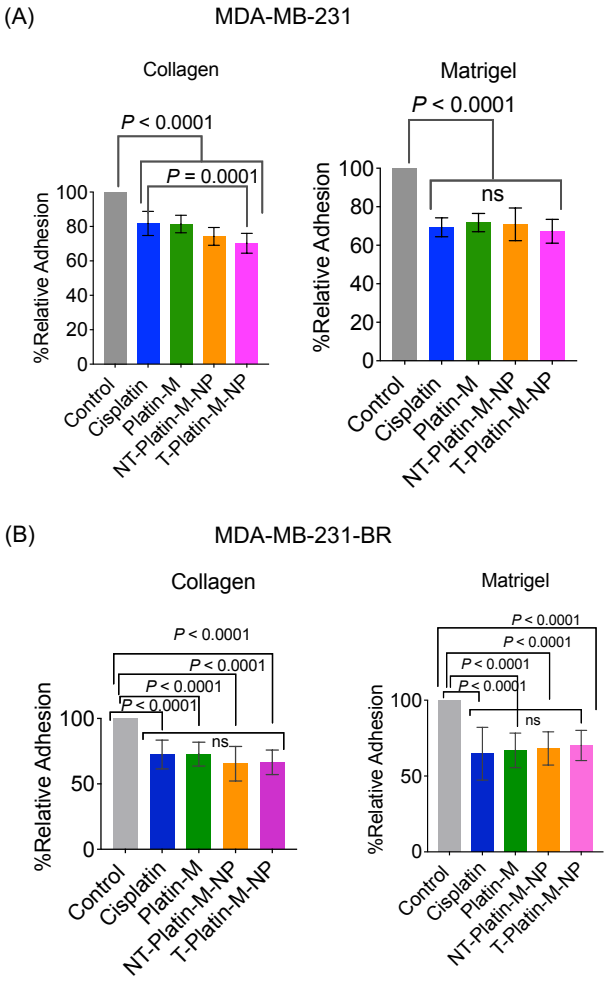

Figure S23. Effect of test articles on adhesion ability of (A) MDA-MB-231 and (B) MDA-MB-231-BR cells. [Cisplatin]: 10 μM, [Platin-M]: 10 μM, and concentration of T-Platin-M-NP or NT-Platin-M-NP was calculated with respect to [Platin-M]: 10 μM. Statistical analyses were performed using ordinary one-way ANOVA with multiple comparison.

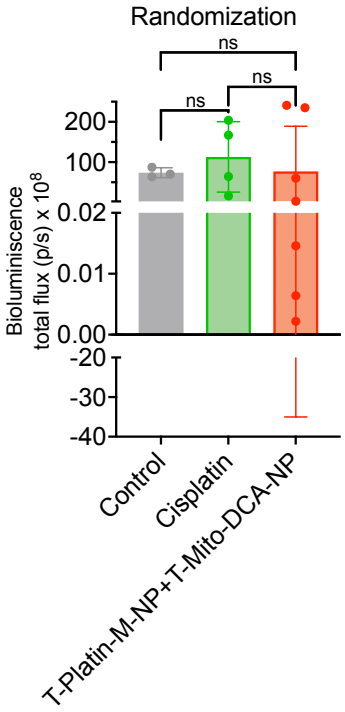

Figure S24. Data illustrating the randomization of animals based on primary tumor bioluminescence before conducting orthotopic stereotactic implantation in brain for the efficacy study of combinatorial nanoparticles in the dual tumor model.

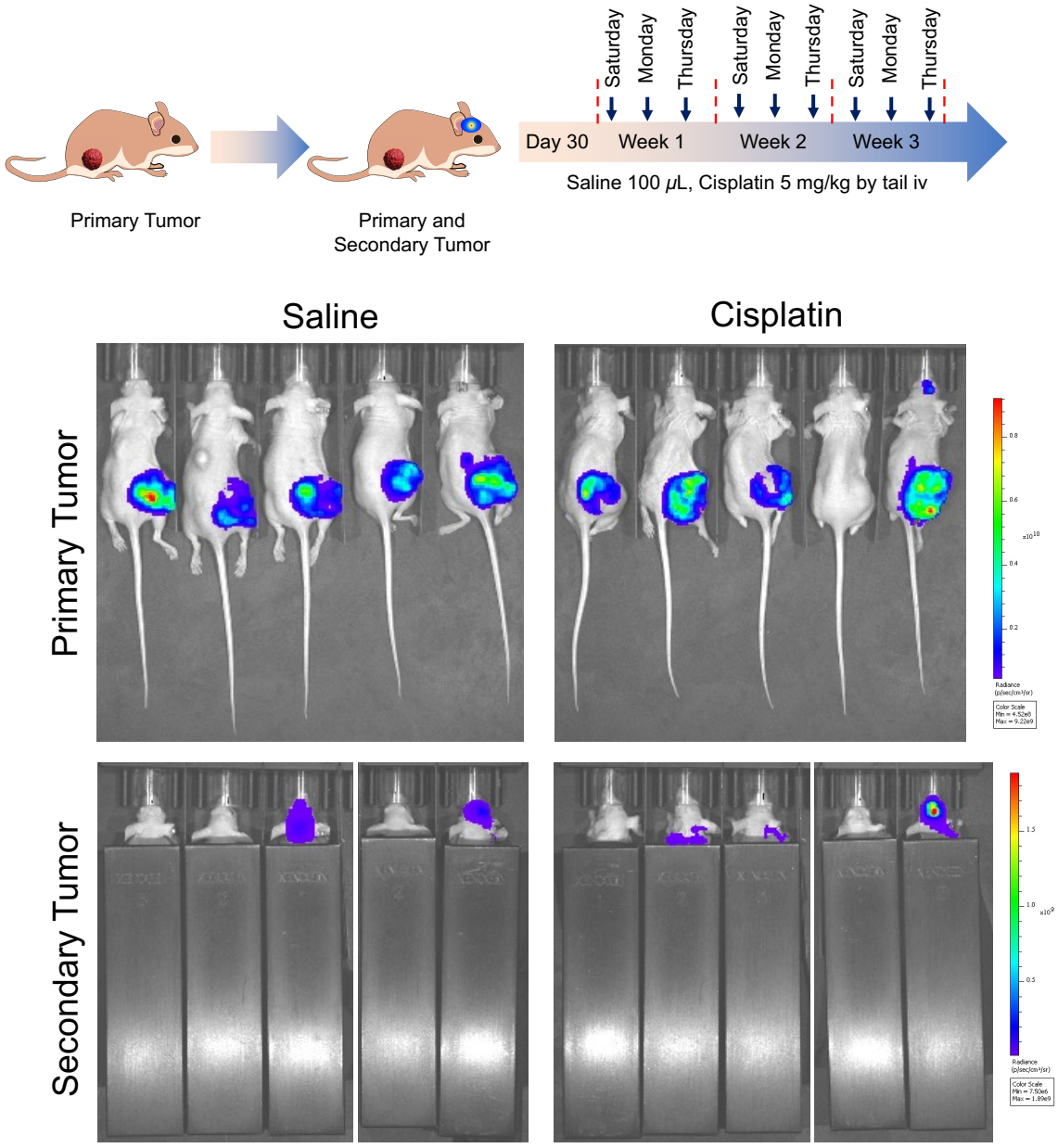

Figure S25. Effects of cisplatin in a dual tumor model. (Top) A schematic diagram of the experimental details. (Bottom) A representative comparison of animals from cisplatin and saline treated groups by IVIS imaging predose and on terminal day of the study.

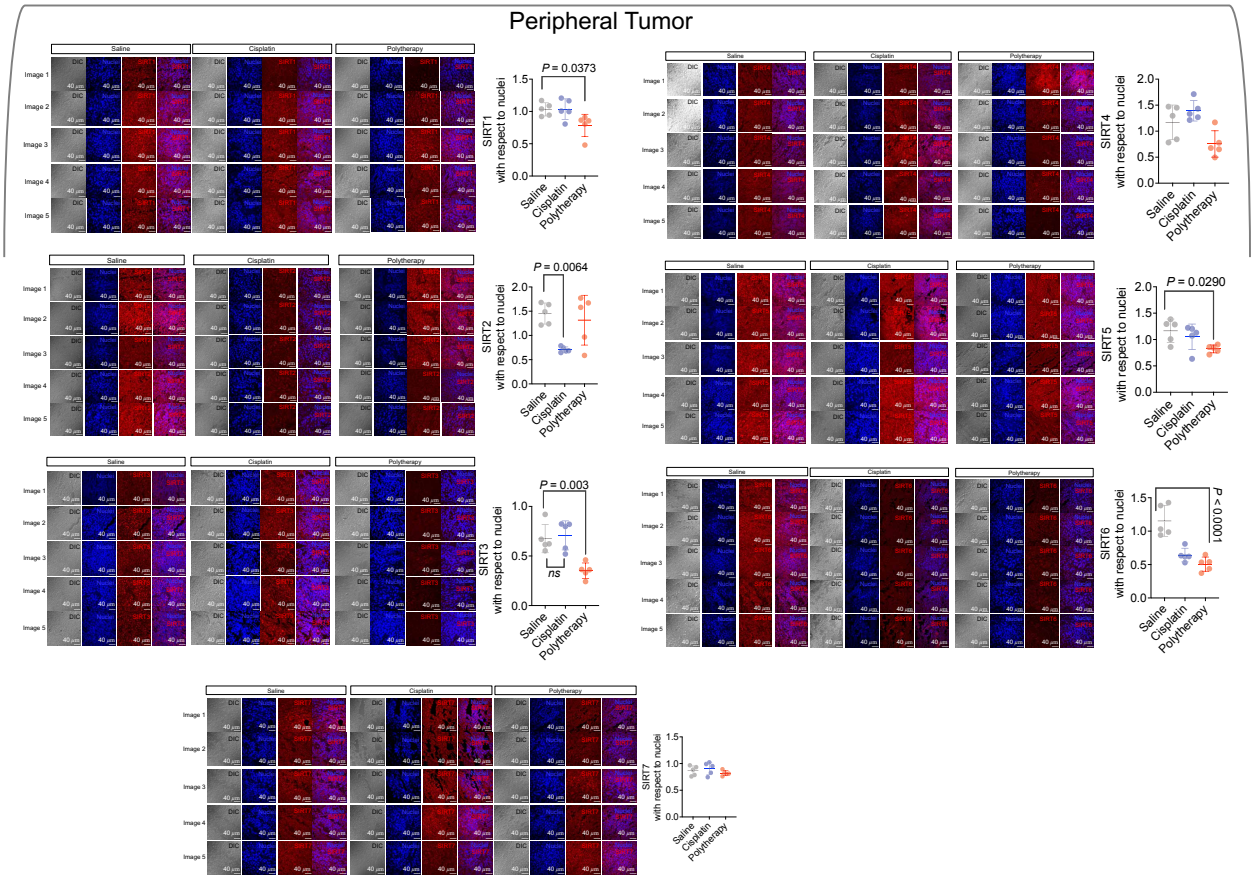

Figure S26. Immunofluorescence images revealing the change in expression of all the sirtuin proteins (SIRT1-7) with respect to nuclei in peripheral tumor tissue upon treatment with a combination of T-Platin-M-NP and T-Mito-DCA-NP compared to saline and cisplatin. The combination therapy is termed here as polytherapy. All images were quantified using the mean intensity values from the protein of interest with respect to the mean intensity of nuclei using ImageJ software. Ordinary one-way analysis of variance (ANOVA) was used to depict the statistical significance between the groups.

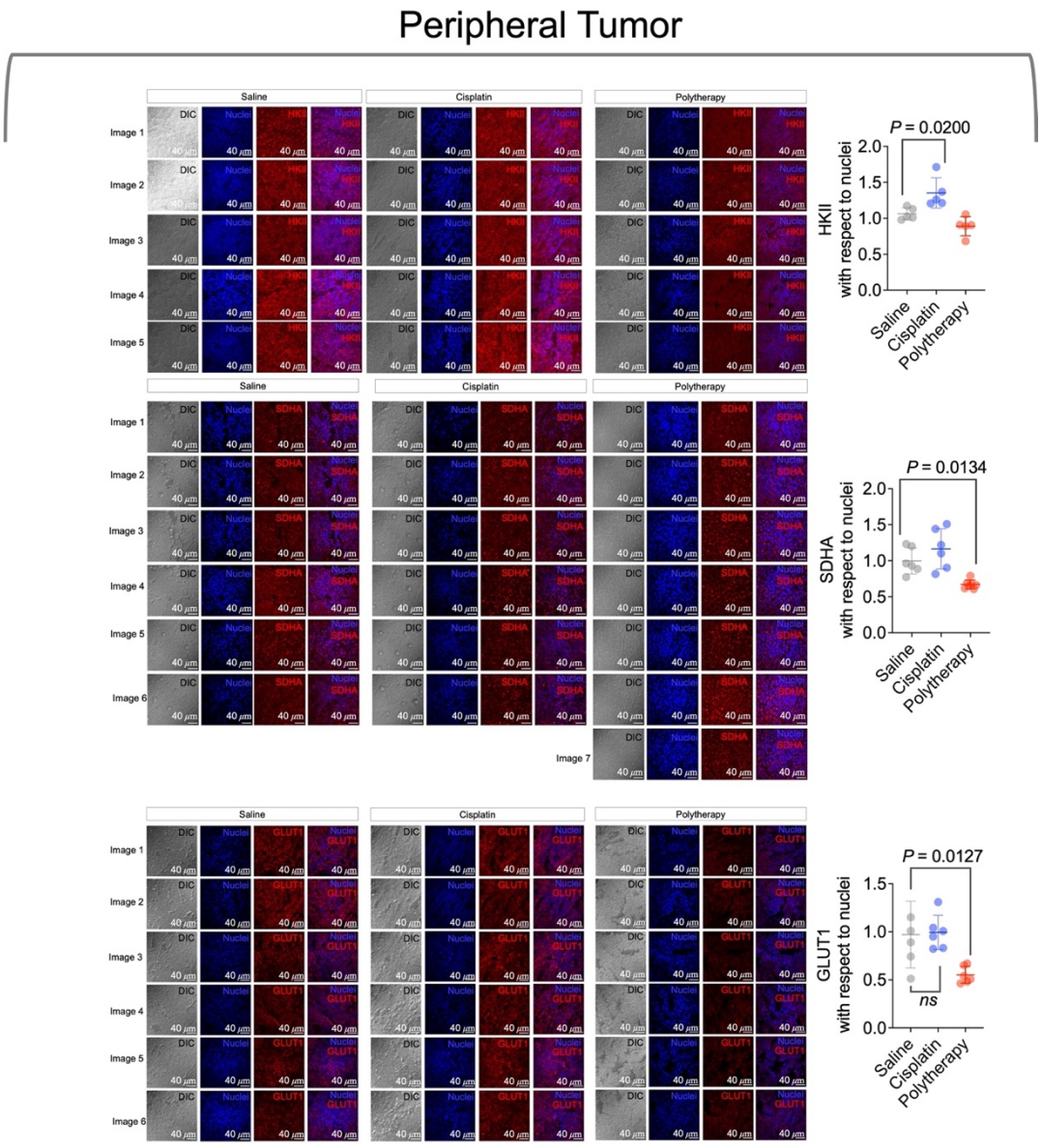

Figure S27. Immunofluorescence images revealing the change in expression of glycolytic proteins HKII and GLUT1 and OXPHOS related protein SDHA with respect to nuclei in peripheral tumor tissue upon treatment with a combination of T-Platin-M-NP and T-Mito-DCA-NP compared to saline and cisplatin. The combination therapy is termed here as polytherapy. All images were quantified using the mean intensity values from the protein of interest with respect to the mean intensity of nuclei using ImageJ software. Ordinary one-way analysis of variance (ANOVA) was used to depict the statistical significance between the groups.

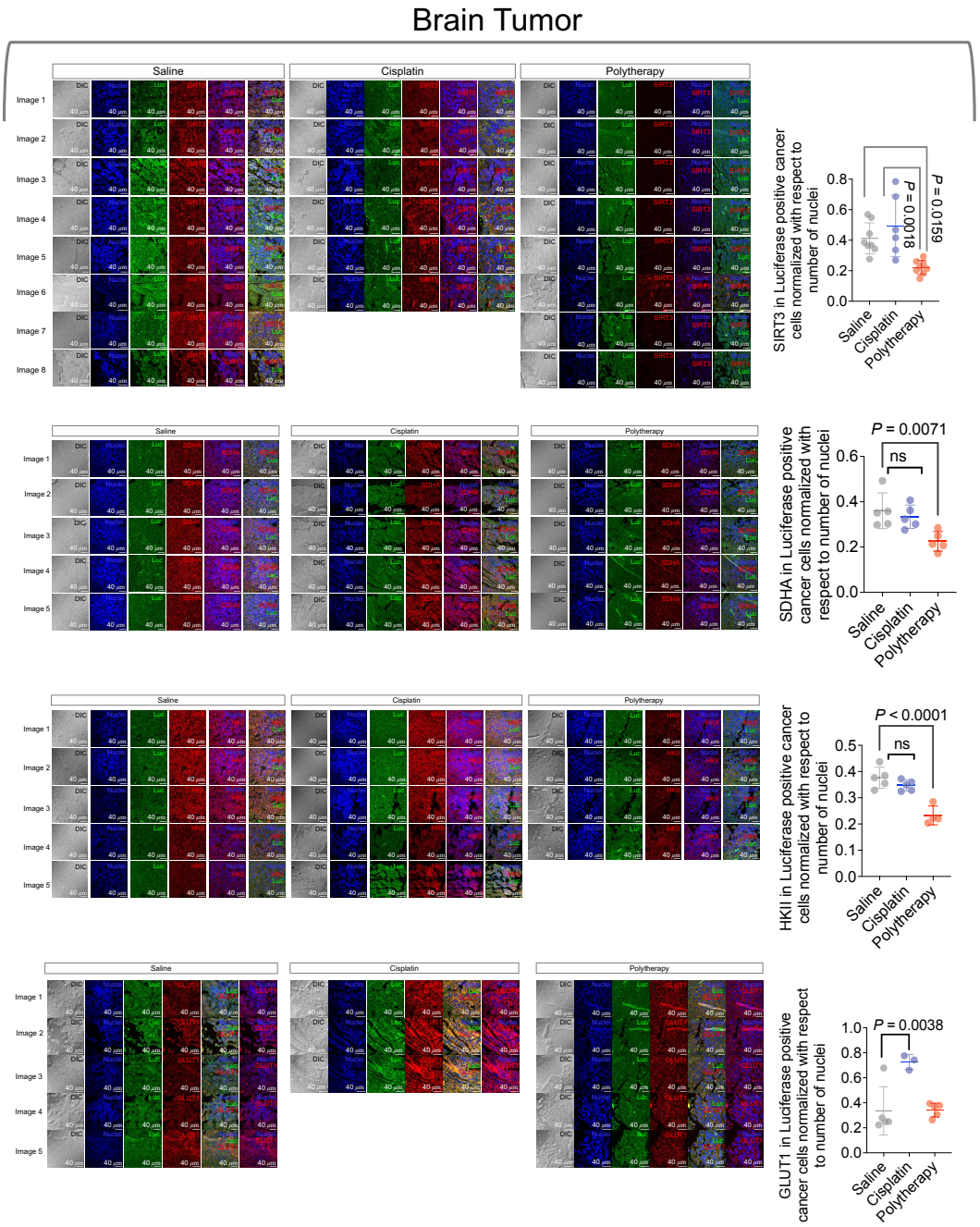

Figure S28. Immunofluorescence images revealing the change in expression of SIRT3, glycolytic proteins HKII and GLUT1, and OXPHOS related protein SDHA in luciferase positive cells with respect to the number of nuclei in brain tumor tissue upon treatment with a combination of T-Platin-M-NP and T-Mito-DCA-NP compared to saline and cisplatin. The combination therapy is termed here as polytherapy. All images were quantified using the mean intensity values from the protein of interest in luciferase positive cells with respect to the number of nuclei using ImageJ software. Ordinary one-way analysis of variance (ANOVA) was used to depict the statistical significance between the groups.

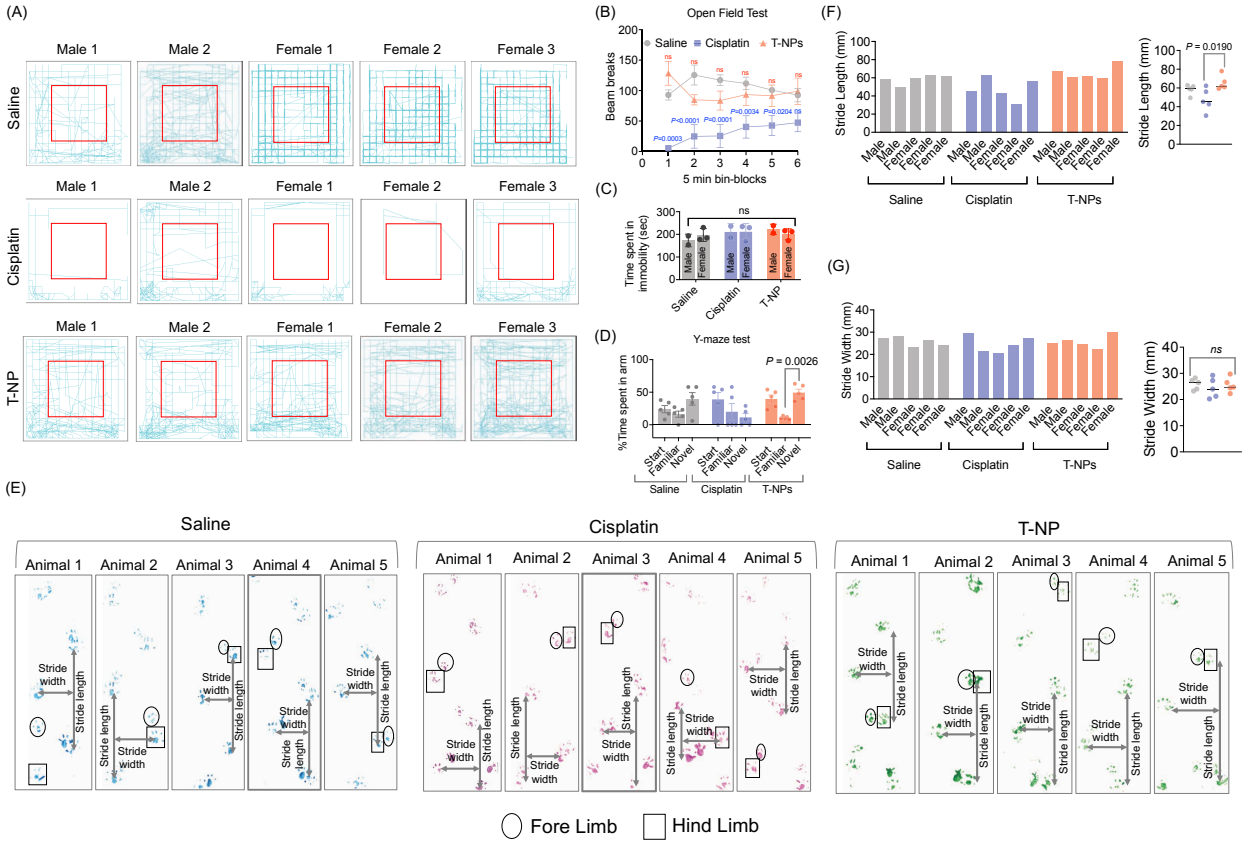

Figure S29. Neurocognitive responses post treatment with T-NPs. (A) Trace path from the open field test showing the locomotion pattern of the animals in saline, cisplatin, and T-NPs treated group. (B) Scatter plot showing the number of beam breaks corresponding to each 5 min bin-blocks from the open field test. (C) Tail suspension test revealing no significant difference in the time spent in immobility across saline, cisplatin, and T-NPs treated groups, suggesting no depression-like behavior due to treatment. (D) Y-maze test showing the total percentage of time mouse from each group spends in start (S) arm, familiar (F) arm, and novel (N) arm. A significant increase in willingness to explore 'N' arm was observed in the T-NPs treated mice, suggesting improved neurocognition. (E) Trace path images from the foot placement study showing the locomotor pattern of the mice and measurements of stride length (mm) (F) and stride width (mm) (G) from the respective trace paths. The data for stride length of each animal is represented as the mean from a minimum of 3 stride length measurements and the data for stride width is represented as the mean from 4 stride width measurements. The average data from all animals are presented on the right of F and G. The study was performed in N = 15 BALB/c albino mice were randomly distributed in 3 groups each with 5 mice (2 male and 3 female). Group 1 was administered with 100 μL saline, group 2 was administered with 5 mg/kg per dose cisplatin twice weekly for 4 weeks, and group 3 the mice were injected with T-NPs at 300 mg/kg per dose, biweekly for 4 weeks. The cumulative dose of T-NPs was 2400 mg/kg. All the test articles were injected through tail i.v. route. The statistical significance was determined by 2way analysis of variance (ANOVA) test.

Figure S30. Representation of measurements conducted in foot placement study. For each animal, the stride length was measured as the distance in millimeters between the hind limbs of the successive foot placements. The stride width was measured as the distance in millimeters between the left and right hind limbs. The data for stride length of each animal is represented as the mean from a minimum of 3 stride length measurements and the data for stride width is represented as the mean from 4 stride width measurements.

References

1. Marrache, S.; Dhar, S., Engineering of blended nanoparticle platform for delivery of mitochondria-acting therapeutics. *Proceedings of the National Academy of Sciences* **2012,** *109* (40), 16288-16293.
2. Marrache, S.; Pathak, R. K.; Dhar, S., Detouring of cisplatin to access mitochondrial genome for overcoming resistance. *Proceedings of the National Academy of Sciences* **2014,** *111* (29), 10444-10449.
3. Pathak, R. K.; Marrache, S.; Harn, D. A.; Dhar, S., Mito-DCA: A Mitochondria Targeted Molecular Scaffold for Efficacious Delivery of Metabolic Modulator Dichloroacetate. *ACS Chemical Biology* **2014,** *9* (5), 1178-1187.
4. Surnar, B.; Basu, U.; Banik, B.; Ahmad, A.; Marples, B.; Kolishetti, N.; Dhar, S., Nanotechnology-mediated crossing of two impermeable membranes to modulate the stars of the neurovascular unit for neuroprotection. *Proceedings of the National Academy of Sciences* **2018,** *115* (52), E12333-E12342.
5. Kolb, D.; Kolishetti, N.; Surnar, B.; Sarkar, S.; Guin, S.; Shah, A. S.; Dhar, S., Metabolic Modulation of the Tumor Microenvironment Leads to Multiple Checkpoint Inhibition and Immune Cell Infiltration. *ACS Nano* **2020,** *14* (9), 11055-11066.
6. Surnar, B.; Shah, A. S.; Park, M.; Kalathil, A. A.; Kamran, M. Z.; Ramirez Jaime, R.; Toborek, M.; Nair, M.; Kolishetti, N.; Dhar, S., Brain-Accumulating Nanoparticles for Assisting Astrocytes to Reduce Human Immunodeficiency Virus and Drug Abuse-Induced Neuroinflammation and Oxidative Stress. *ACS Nano* **2021,** *15* (10), 15741-15753.
7. Ewing, B.; Hillier, L.; Wendl, M. C.; Green, P., Base-calling of automated sequencer traces usingPhred. I. Accuracy assessment. *Genome Res.* **1998,** *8* (3), 175-185.
8. Kim, D.; Langmead, B.; Salzberg, S. L., HISAT: a fast spliced aligner with low memory requirements. *Nat. Methods.* **2015,** *12* (4), 357-360.
9. McKenna, A.; Hanna, M.; Banks, E.; Sivachenko, A.; Cibulskis, K.; Kernytsky, A.; Garimella, K.; Altshuler, D.; Gabriel, S.; Daly, M., The Genome Analysis Toolkit: a MapReduce framework for analyzing next-generation DNA sequencing data. *Genome Res.* **2010,** *20* (9), 1297-1303.
10. Pertea, M.; Pertea, G. M.; Antonescu, C. M.; Chang, T.-C.; Mendell, J. T.; Salzberg, S. L., StringTie enables improved reconstruction of a transcriptome from RNA-seq reads. *Nat. Biotechnol.* **2015,** *33* (3), 290-295.
11. Trapnell, C.; Williams, B. A.; Pertea, G.; Mortazavi, A.; Kwan, G.; Van Baren, M. J.; Salzberg, S. L.; Wold, B. J.; Pachter, L., Transcript assembly and quantification by RNA-Seq reveals unannotated transcripts and isoform switching during cell differentiation. *Nat. Biotechnol.* **2010,** *28* (5), 511-515.
12. Florea, L.; Song, L.; Salzberg, S. L., Thousands of exon skipping events differentiate among splicing patterns in sixteen human tissues. *F1000Research* **2013,** *2*.
13. Jiang, H.; Wong, W. H., Statistical inferences for isoform expression in RNA-Seq. *Bioinformatics* **2009,** *25* (8), 1026-1032.
14. Eddy, S. R., Profile hidden Markov models. *Bioinformatics (Oxford, England)* **1998,** *14* (9), 755-763.
15. Xie, C.; Mao, X.; Huang, J.; Ding, Y.; Wu, J.; Dong, S.; Kong, L.; Gao, G.; Li, C.-Y.; Wei, L., KOBAS 2.0: a web server for annotation and identification of enriched pathways and diseases. *Nucleic Acids Res.* **2011,** *39* (suppl_2), W316-W322.
16. Kanehisa, M.; Goto, S.; Kawashima, S.; Okuno, Y.; Hattori, M., The KEGG resource for deciphering the genome. *Nucleic Acids Res.* **2004,** *32* (suppl_1), D277-D280.
17. Finn, R. D.; Bateman, A.; Clements, J.; Coggill, P.; Eberhardt, R. Y.; Eddy, S. R.; Heger, A.; Hetherington, K.; Holm, L.; Mistry, J., Pfam: the protein families database. *Nucleic Acids Res.* **2014,** *42* (D1), D222-D230.

18. Koonin, E. V.; Fedorova, N. D.; Jackson, J. D.; Jacobs, A. R.; Krylov, D. M.; Makarova, K. S.; Mazumder, R.; Mekhedov, S. L.; Nikolskaya, A. N.; Rao, B. S., A comprehensive evolutionary classification of proteins encoded in complete eukaryotic genomes. *Genome Biol.* **2004,** *5* (2), 1-28.
19. Tatusov, R. L.; Galperin, M. Y.; Natale, D. A.; Koonin, E. V., The COG database: a tool for genome-scale analysis of protein functions and evolution. *Nucleic Acids Res.* **2000,** *28* (1), 33-36.
20. Ashburner, M.; Ball, C. A.; Blake, J. A.; Botstein, D.; Butler, H.; Cherry, J. M.; Davis, A. P.; Dolinski, K.; Dwight, S. S.; Eppig, J. T., Gene ontology: tool for the unification of biology. *Nat. Genet.* **2000,** *25* (1), 25-29.
21. Apweiler, R.; Bairoch, A.; Wu, C. H.; Barker, W. C.; Boeckmann, B.; Ferro, S.; Gasteiger, E.; Huang, H.; Lopez, R.; Magrane, M., UniProt: the universal protein knowledgebase. *Nucleic Acids Res.* **2004,** *32* (suppl_1), D115-D119.
22. Deng, Y.; Li, J.; Wu, S.; Zhu, Y.; Chen, Y.; He, F., Integrated nr database in protein annotation system and its localization. *Comput. Eng.* **2006,** *32* (5), 71-74.
23. Altschul, S. F.; Madden, T. L.; Schäffer, A. A.; Zhang, J.; Zhang, Z.; Miller, W.; Lipman, D. J., Gapped BLAST and PSI-BLAST: a new generation of protein database search programs. *Nucleic Acids Res.* **1997,** *25* (17), 3389-3402.
24. Djebali, S.; Davis, C. A.; Merkel, A.; Dobin, A.; Lassmann, T.; Mortazavi, A.; Tanzer, A.; Lagarde, J.; Lin, W.; Schlesinger, F., Landscape of transcription in human cells. *Nature* **2012,** *489* (7414), 101-108.
25. Andrews, S., FastQC: a quality control tool for high throughput sequence data. Babraham Bioinformatics, Babraham Institute, Cambridge, United Kingdom: 2010.
26. Chen, S.; Zhou, Y.; Chen, Y.; Gu, J., fastp: an ultra-fast all-in-one FASTQ preprocessor. *Bioinformatics* **2018,** *34* (17), i884-i890.
27. Kawakami, M.; Kawakami, K.; Puri, R. K., Intratumor administration of interleukin 13 receptor-targeted cytotoxin induces apoptotic cell death in human malignant glioma tumor xenografts. *Mol. Cancer Ther.* **2002,** *1* (12), 999-1007.
28. Putri, G. H.; Anders, S.; Pyl, P. T.; Pimanda, J. E.; Zanini, F., Analysing high-throughput sequencing data in Python with HTSeq 2.0. *Bioinformatics* **2022,** *38* (10), 2943-2945.
29. Eddy, S. R., A new generation of homology search tools based on probabilistic inference. In *Genome Informatics 2009: Genome Informatics Series Vol. 23*, World Scientific: 2009; pp 205-211.
30. Kang, C.-H.; So, J.-S., Antibiotic and heavy metal resistance in Shewanella putrefaciens strains isolated from shellfishes collected from West Sea, Korea. *Mar. Pollut. Bull.* **2016,** *112* (1-2), 111-116.
31. Huerta-Cepas, J.; Forslund, K.; Coelho, L. P.; Szklarczyk, D.; Jensen, L. J.; Von Mering, C.; Bork, P., Fast genome-wide functional annotation through orthology assignment by eggNOG-mapper. *Mol. Biol. Evol.* **2017,** *34* (8), 2115-2122.
32. Wu, T.; Hu, E.; Xu, S.; Chen, M.; Guo, P.; Dai, Z.; Feng, T.; Zhou, L.; Tang, W.; Zhan, L., clusterProfiler 4.0: A universal enrichment tool for interpreting omics data. *Innov.* **2021,** *2* (3), 100141.
33. Aramaki, T.; Blanc-Mathieu, R.; Endo, H.; Ohkubo, K.; Kanehisa, M.; Goto, S.; Ogata, H., KofamKOALA: KEGG Ortholog assignment based on profile HMM and adaptive score threshold. *Bioinformatics* **2020,** *36* (7), 2251-2252.